RSC Sustainability

ROYAL SOCIETY OF CHEMISTRY

CRITICAL REVIEW

View Article Online
View Journal | View Issue

Cite this: *RSC Sustainability*, 2025, **3**, 5027

Natural polymer-based bioadsorbents for wastewater treatment

Akhtar Alam, *[a] Atikur Hassan, [b] Zernain Sultana[a] and Neeladri Das *[b]

Received 23rd May 2025
Accepted 26th September 2025

DOI: 10.1039/d5su00369e

rsc.li/rscsus

Due to rapid urbanization, industrial growth, and rising living standards, the intensification of global water pollution has become a pressing environmental and public health challenge. Effective and sustainable treatment technologies are urgently needed to mitigate these threats. Adsorption is a well-known, effective and sustainable approach because it is simple to operate, cost-effective, and highly efficient. In this context, porous materials derived from natural biopolymers have gained prominence as super-adsorbents for wastewater treatment due to their renewable origin, biodegradability and environmental compatibility. Biopolymers such as cellulose, chitosan, alginate, starch, and gelatin are often functionalized with electron-rich atoms such as nitrogen (N), oxygen (O), sulfur (S), metals, or fillers. These biopolymers exhibit a high affinity for a broad range of pollutants *via* mechanisms such as ion exchange, hydrogen bonding, and surface complexation. Recent advances in hybrid composites have enhanced the mechanical stability, adsorption capacity, and reusability of these materials, enabling them to achieve pollutant removal efficiencies of up to 99%. This review provides an extensive overview of the modification strategies, adsorption mechanisms, and performance metrics of biopolymer-based porous adsorbents.

Sustainability spotlight

Access to clean water and sanitation is an urgent global challenge addressed by United Nations Sustainable Development Goal 6 (SDG 6). Porous materials made from natural biopolymers are an environmentally friendly solution for wastewater treatment due to their sustainability approaches. These materials are derived from renewable sources, including cellulose, chitosan, alginate, and starch. They are characterized by low toxicity, biodegradability, and rich surface functionalities. These properties make them ideal for removing a wide range of contaminants, including dyes, heavy metals, and emerging contaminants. These materials are often synthesized using green chemistry principles, which reduces reliance on toxic reagents and energy-intensive processes. Recent innovations in structure tuning, hybridization, and regeneration have improved their applicability in real-world water systems. Promoting cost-effective, scalable, and environmentally friendly water treatment technologies that use porous biopolymer-based adsorbents significantly advances environmental sustainability. This approach aligns with climate change goals (SDG 13) because it decreases the carbon footprint of traditional treatment processes. Furthermore, these technologies protect aquatic ecosystems (SDG 14) by filtering out harmful pollutants before they enter natural bodies of water.

1. Introduction

The continuous improvement of living standards and the rapid growth in population are driving the development of new industries and technologies at an unprecedented rate.[1] In 2022, roughly 2.2 billion people lacked access to safely managed drinking water, and 42% of household wastewater (~113 billion m^3) was not safely treated.[2–5] Looking ahead, global water demand is projected to rise by 20–30% by 2050, driven by population growth, urbanization, and expanding industry and agriculture. Concurrently, wastewater production is expected to increase by ~50% by 2050.[6,7] A wide range of waste pollutants are dumped from various sources, including mining, industrial waste from electronic devices, chemicals, pharmaceuticals, cosmetics, dyes, textiles, oil refining, petrochemicals, fertilizers, pesticides, paints, and paper printing.[8–18] However, most of these wastes are toxic in nature and even carcinogenic to microbial populations and also difficult to degrade. As a result, water resources are deteriorating on a daily basis on a global scale due to the contamination of such immense quantities of hazardous waste, particularly heavy metal ions, minerals, toxic dyes, organic impurities, and pharmaceutical poisons.[19–22] This issue has become a grave concern for human health and the natural environment, as water is indispensable for life.[23–25] Table 1 provides different types of water pollutants and their respective impacts. For instance, numerous toxic metal ions, especially Cu^{2+} (copper), As (arsenic), Co^{2+} (cobalt), Ni^{2+} (nickel), Cd^{2+} (cadmium), Zn^{2+} (zinc), Hg^{2+} (mercury), Pb^{2+} (lead), and Cr^{4+}/Cr^{6+} (chromium), can produce harmful effects on our environment.[26–30] These toxic metal ions can accumulate in our bodies through food and water and damage several organs and

[a]*Department of Chemical Sciences, Bose Institute, Kolkata – 700091, India. E-mail: akhtar.alam@jcbose.ac.in*

[b]*Department of Chemistry, Indian Institute of Technology Patna, Patna – 801106, India. E-mail: neeladri@iitp.ac.in; neeladri2002@yahoo.co.in*

tissues, such as the kidneys, liver, eyes, skin, gastrointestinal tract, and central nervous system.[31] On the other hand, the presence of toxic dyes such as methylene blue (MB), Congo red (CR), methyl orange (MO), rhodamine B (RB), malachite green (MG), and crystal violet (CV) in water might pose serious risks to humans and aquatic communities.[32,33] Organic micro-pollutants, such as cyanides, phosphates, phenols, petroleum oils, and pharmaceutical waste, have been recognized as hazardous to the ecosystem when present in water.[34] To avoid the negative effects on the environment and human health, it is necessary to remove these toxic pollutants from contaminated water before discharging.[35]

A variety of conventional methods have been established for removing toxic pollutants from wastewaters. These methods include precipitation, coagulation, evaporation, distillation, oxidation, electrolysis, reverse osmosis, ion exchange, filtration and adsorption.[36–38] Conventional wastewater treatment methods, while widely used, face numerous limitations that impact their efficiency and sustainability. Precipitation, which converts dissolved contaminants into solids, generates large amounts of sludge and needs strict pH control, yet struggles with low pollutant concentrations.[39,40] Coagulation, using chemicals like alum or ferric salts, also creates sludge and is highly dependent on water chemistry.[41–43] Thermal methods like evaporation and distillation are energy-intensive, costly, and unsuitable for heat-sensitive compounds due to fouling and degradation risks.[44–46] Oxidation processes rely on hazardous chemicals that can produce toxic by-products, while electrolysis consumes a lot of energy, causes electrode wear, and is less effective for complex waste streams.[47–50] Reverse osmosis, though effective, suffers from membrane fouling, high energy costs, and reject water disposal issues. Ion exchange is limited by high material costs and low selectivity.[51–55] Additionally, filtration only removes suspended solids, not dissolved contaminants, and it requires frequent maintenance.[56–58] These drawbacks emphasize the urgent need for more sustainable, cost-effective, and environmentally friendly treatment options, such as adsorption.[59–67]

Akhtar Alam

Dr Akhtar Alam received his PhD degree in Chemistry from the Department of Chemistry at the Indian Institute of Technology Patna (IIT Patna) in March 2022. He thereafter worked as a postdoctoral research fellow in the Department of Chemical and Biological Sciences at the S. N. Bose National Centre for Basic Sciences, Kolkata, India. Currently, he is working as an DST INSPIRE Faculty Fellow at the Bose Institute, Kolkata, India. His ongoing research interests focus on the design and synthesis of novel covalent organic frameworks for photocatalytic organic transformation, water splitting and hydrogen peroxide generation.

Atikur Hassan

Atikur Hassan received his Bachelor's and Master's degrees in Chemistry from Aligarh Muslim University (India). He joined the Indian Institute of Technology Patna as a research fellow under the supervision of Dr Neeladri Das. He was awarded a PhD degree in 2024. He is currently working as a Postdoctoral Researcher in the Department of Chemistry at KU Leuven, Belgium. His research focuses on designing advanced functional porous materials for applications in energy and environmental sustainability.

Zernain Sultana

Zernain Sultana is currently pursuing her PhD in the Department of Chemical Sciences at the Bose Institute, Kolkata. She received her Master of Science (MSc) degree in Organic Chemistry from West Bengal State University, India. She also completed her Bachelor of Science (BSc) in Chemistry from the same university. Her research focuses primarily on the synthesis of bioactive molecules and natural products, with a particular emphasis on designing carbohydrate-based therapeutic agents.

Neeladri Das

Dr Neeladri Das received his PhD in Chemistry from the University of Utah, USA, in 2007 under the supervision of Professor Peter J. Stang. He is currently an Associate Professor in the Department of Chemistry at the Indian Institute of Technology Patna, India. Dr Das' research interests primarily focus on the development of advanced functional porous materials, including porous organic polymers (POPs), covalent organic frameworks (COFs), and coordination-driven metallacycles for environmental, catalytic, and biological applications.

Table 1 Lists of different types of water pollutants and their respective impacts

Type of pollutant	Examples	Primary sources	Environmental/health impacts	Ref.
Inorganic pollutants	Heavy metals (Pb, Cd, Cr(VI), As, Hg, Ni, Cu, Zn); nutrients (nitrates, phosphates, and fluorides)	Mining, electroplating, fertilizer runoff, pesticides, and industrial effluents	Bioaccumulation, carcinogenic/mutagenic effects, kidney/liver damage, and eutrophication	68–71
Organic pollutants	Synthetic dyes (azo, anthraquinone, indigo), pharmaceuticals (antibiotics, hormones, analgesics), pesticides (DDT, organophosphates), phenols, PAHs, VOCs	Textile dyeing, pharmaceutical waste, agrochemicals, petrochemical industries, and oil spills	Endocrine disruption, antibiotic resistance, aquatic toxicity, carcinogenic risks	72–83
Biological pollutants	Bacteria (*E. coli*, *Vibrio cholerae*), viruses (hepatitis, rotavirus), protozoa (*Giardia*, *Cryptosporidium*), helminths, cyanobacteria	Untreated sewage, hospital waste, agricultural runoff, contaminated drinking water	Waterborne diseases (cholera, dysentery, hepatitis), algal toxin release, and ecosystem imbalance	84–88
Emerging contaminants	Microplastics, nanoplastics, endocrine-disrupting chemicals (BPA, phthalates), and personal care products	Plastic degradation, cosmetics, detergents, industrial nanotechnology, and packaging waste	Persistent in ecosystems, bioaccumulation, hormonal disruption, and chronic ecological effects	72 and 89–94
Other physical pollutants	Suspended solids (silt, clay, colloids), thermal pollution, salinity, turbidity, and radioactive isotopes	Soil erosion, construction runoff, power plant cooling water, mining, and nuclear waste	Reduced light penetration, oxygen depletion, altered aquatic habitats, and radiological risks	95–99

Nevertheless, adsorption using a solid adsorbent is regarded as the best approach among the various available methods because it is a simple, efficient and inexpensive technique.[100–107] Adsorption involves trapping pollutants on the surface of solid materials, and it is widely recognized for its simplicity and effectiveness.[108–114] Of particular note, it is a conventional one that is associated with the capacity for regeneration and facilitating large-scale applications. Indeed, varieties of inorganic adsorbents have been used for the removal of toxic contaminants from wastewaters. Some examples are activated carbon, silica, zeolites, metal oxides, and clay minerals.[115–118] However, the utilization of these conventional adsorbents possesses numerous drawbacks, such as limited surface area, diminished adsorption capacities, substantial expenses, and toxicity.[119] Consequently, there is still great research interest in exploring novel adsorbent materials for the effective and efficient removal of toxic pollutants from wastewater.[120,121] From this perspective, several solid porous adsorbents, including synthetic polymers, porous organic polymers (POPs), covalent organic frameworks (COFs), organic–inorganic hybrid polymers, polymeric composites, metal–organic polymers (MOFs), and graphene-based nanomaterials have been reported for wastewater treatment.[122–126] However, many drawbacks limit their use to the laboratory level, which include high cost, time-consuming treatment, lower adsorption capacity, difficulty in synthesizing on a large scale, non-selectivity and lack of reusability.[127–130] As promising adsorbents for removing water contaminants, materials should not only have good adsorption capacity and feasibility, but also the ability to easily desorb the adsorbed molecules/ions, making them efficiently recyclable and reusable for several times. Therefore, in order to treat industrial wastewater in an economical and efficient manner, it is imperative to utilize an appropriate adsorbent that fulfills the requisite criteria, including elevated adsorption capacity, selectivity, rapid adsorption kinetics, multiple absorbability, and productivity.[130,131]

In recent years, natural biopolymer-based materials have been the focus of considerable interest because of their unique properties, including physicochemical stability, improved surface area, biodegradability, affordability, non-toxicity and environmental sustainability.[132,133] Hence, the development of ecofriendly functionalized biopolymer-based materials could be a great choice for removal of various toxic pollutants especially heavy metals or inorganic ions, toxic dyes, hazardous organic and pharmaceutical compounds.[134] A variety of naturally occurring biopolymers, including cellulose, chitosan, alginate, gelatin, starch, and carrageenan, have been identified as highly effective adsorbents for eliminating water pollutants.[135] These biopolymers are widely available and exhibit remarkable structural diversity, making them promising super adsorbents for water remediation (Fig. 1). Contemporary research has developed several biopolymer-based adsorbents in the form of composites, blends, aerogels, hydrogels, foams, fibers, films, and membranes by incorporating activated carbon, carbon nanotubes, silica, clay, zeolite, graphene, metal nanoparticles, and synthetic or natural polymers. This review provides an overview of the most recent synthesis and advancements in a variety of cutting-edge biopolymer-based adsorbents for the

remediation of noxious industrial effluents, including metal ions, textile dyes, micropollutants of an organic nature and pharmaceutical impurities. In order to evaluate an efficient adsorbent in related applications, the adsorption process must be understood. Thus, to this end, the important parameters such as theoretical equations, adsorption isotherms, adsorption kinetic models, and adsorption thermodynamics have been considered.

2. Understanding adsorption: theories and mechanisms

Adsorption is a process in which molecules of a gas/liquid referred to as the adsorbate adhere to the surface of a solid/liquid referred to as the adsorbent (Fig. 2a). Unlike absorption, which involves penetration and integration into the bulk of the material, adsorption occurs solely at the surface, forming a thin film of the adsorbate. Adsorption techniques are used a lot for all kinds of water treatment, capturing and storing small gases (such as N_2, CO_2, H_2 and CH_4) – evaluating the surface area and pore size of various porous materials, including industrial adsorbents, catalysts and building materials.[136,137] Depending on the interactions between the adsorbate and the adsorbent, adsorption can be termed physisorption or chemisorption.[138] In physisorption, adsorbed molecules or ions are attached *via* weak, reversible van der Waals forces. In contrast, chemisorption occurs primarily through irreversible covalent or electrostatic bonds. The most crucial needs of an effective and efficient adsorbent are affordable, non-poisonous, biocompatible, good physiochemical stability, large specific surface area, high adsorption capacity with a high rate, high selectivity and reusability. Several factors may influence the adsorption capability, including the initial concentration of the adsorbate, the dosage of the adsorbent, temperature, contact time, and the pH of the solution.

In order to investigate the mechanism of adsorption using solid adsorbents, different approaches and theoretical models were frequently employed in terms of isotherms, kinetics, and thermodynamics.[139] The adsorption of water pollutants (adsorbates) takes place in two different states, at the surface and interstices of the adsorbents (Fig. 2b).[140] In surface adsorption, the adsorbate molecules or ions are attracted to a solid surface from an aqueous medium *via* van der Waals forces, dipole interactions, or hydrogen bonding. In contrast, interstitial adsorption involves the diffusion of adsorbate molecules or ions into the adsorbent material, entering its pores, which can be micro, meso, or macro in size.[141] In this context, the use of natural bioadsorbents with electron-rich, active functional groups (*e.g.*, amino, hydroxyl, carboxyl, and thiol groups), high surface area and defined pore size facilitates the efficient capture, adsorption, and binding of positively charged molecules and ions from wastewater systems.[142] To further understand the adsorption mechanism, some theoretical equations/parameters, adsorption isotherms, kinetic models and adsorption thermodynamics have been described concisely.

2.1. Adsorption isotherms

Adsorption isotherm shows the relationship between the amount of adsorbate absorbed by the adsorbent at equilibrium based on its concentration (if adsorbate is in the liquid phase) or pressure (if gas) at constant temperature. In the past few decades, several mathematical models have been developed for evaluating adsorption capacity, including Langmuir, Freundlich, Tempkin, Brunauer–Emmett–Teller, Dubinin–Radushkevich, and Flory–Huggins equilibrium adsorption isotherms.[143] The equilibrium adsorption capacity (Q_e) and the removal efficiency (%R) can be calculated using eqn (1) and (2) for varying concentrations of the adsorbate solution.

$$Q_e = \frac{(C_0 - C_e) \times V}{M} \quad (1)$$

$$\text{Removal efficiency}(\%R) = \frac{C_0 - C_e}{C_e} \times 100\% \quad (2)$$

where the initial concentration of the adsorbate solution is denoted by C_0, the equilibrium concentration by C_e, the volume of the adsorbate solution taken by V, and the weight of the adsorbent charged by M. The Langmuir and Freundlich adsorption isotherm models are frequently employed to estimate the adsorption mechanism of liquid phase solutes by solid adsorbents. The Langmuir isotherm model is defined by eqn (3) and assumes homogeneous formation of a monolayer of adsorbates (*i.e.*, dye molecules), as all non-interacting adsorption sites are anticipated to be energetically identical. In contrast, the Freundlich isotherm model is described by eqn (4) and assumes nonideal, multilayer sorption, wherein all adsorption sites are nonidentical and have different affinities for the adsorbate molecules.

$$\frac{C_e}{Q_e} = \frac{C_e}{Q_m} + \frac{1}{Q_m K_L} \quad (3)$$

$$\ln Q_e = \ln K_F + \frac{1}{n} \ln C_e \quad (4)$$

where Q_e (mg g^{-1}) is the equilibrium adsorption capacity, C_e (mg L^{-1}) the equilibrium concentration, Q_m (mg g^{-1}) the maximum adsorption capacity of the Langmuir isotherm, K_L (L mg^{-1}) is the Langmuir adsorption coefficient, K_F (L mg^{-1}) the Freundlich constant, and $1/n$ is an indicator that describes the nonlinear degree of adsorption.

2.2. Adsorption kinetics

Adsorption kinetic modeling provides valuable insight into the mechanism and reaction pathway of the adsorption reaction, as well as the possible rate-controlling steps. Despite the existence of numerous kinetics models, it is worth noting that two of the most widely adopted models, namely the pseudo-first-order and pseudo-second-order equations, are frequently utilized to elucidate the adsorption kinetics. The pseudo-first-order and pseudo-second-order kinetic models are defined by eqn (5) and (6), respectively.

$$\ln(Q_e - Q_t) = \ln Q_e - k_1 t \quad (5)$$

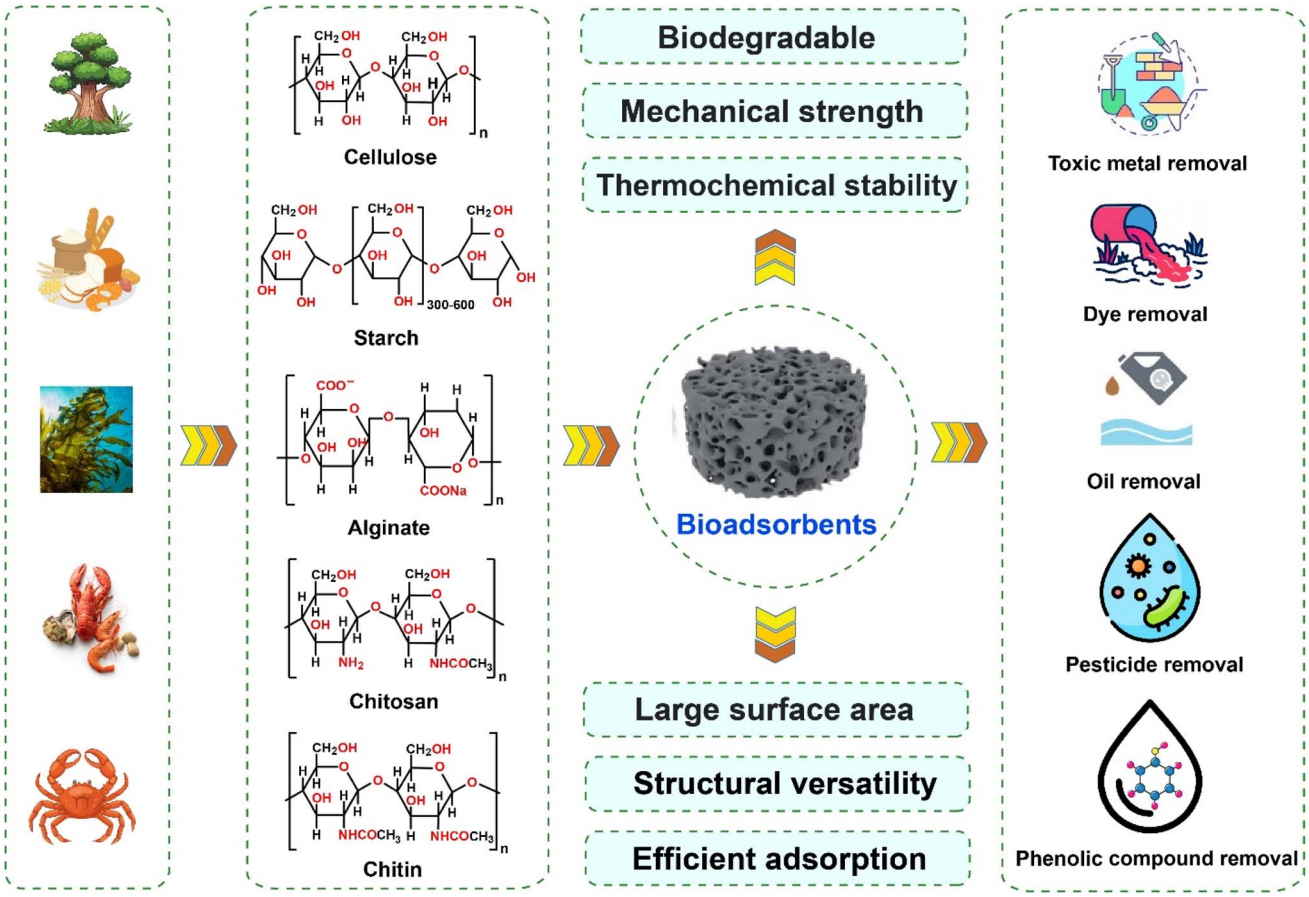

Fig. 1 An overview of the different naturally occurring polymers used in bioadsorbent-based systems for eliminating various pollutants from wastewater.

$$\frac{t}{Q_t} = \frac{1}{k_2 Q_e^{\,2}} + \frac{t}{Q_e} \tag{6}$$

where Q_e is the equilibrium adsorption capacity (mg g^{-1}), Q_t is the adsorption capacity at the t (min) contact time, k_1 (min^{-1}) and k_2 (g mg^{-1} min^{-1}) are the corresponding adsorption rate constants. The activation energy is an integral parameter of the adsorption process because it reveals whether the process is physical or chemical. The activation energy (E_a) can be calculated by using the Arrhenius eqn (7).

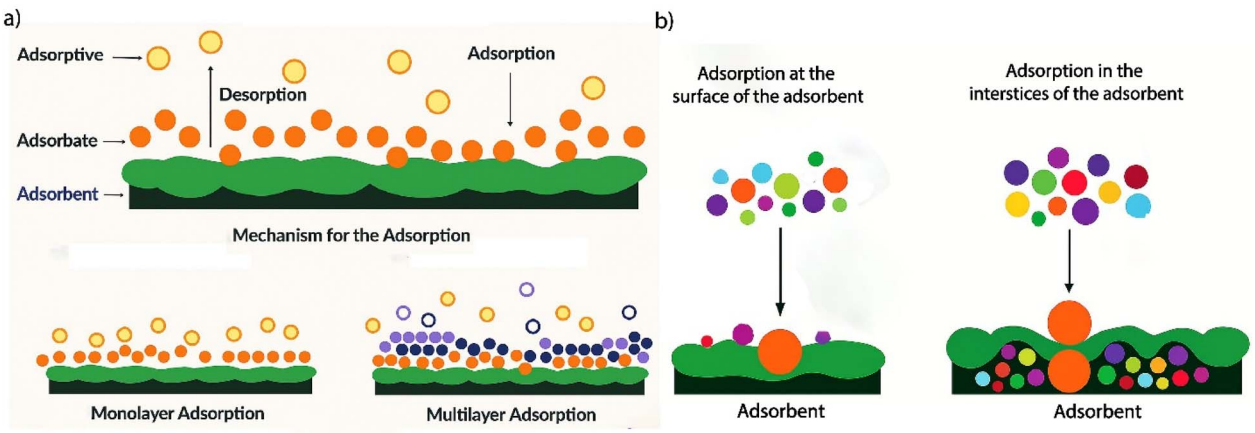

Fig. 2 (a) A schematic illustration of understanding the adsorption and desorption processes and the general mechanism of monolayer and multilayer adsorption. (b) An illustration of the adsorption of adsorbates takes place at the surface and interstices of the adsorbents.

$$\ln k = \ln A - \frac{E_a}{RT} \quad (7)$$

where k is the adsorption rate constant, A is the Arrhenius constant, E_a (kJ mol^{-1}) is the activation energy, R is the ideal gas constant (8.314 J mol^{-1} K^{-1}) and T (K) denotes absolute temperature.

2.3. Adsorption thermodynamics

Thermodynamic studies are also of concern, as temperature exerts a pivotal influence on the adsorption process. These studies provide information about the spontaneity of the adsorption process. The thermodynamic studies are usually evaluated by the temperature being increased or decreased during the adsorption process. To study adsorption thermodynamics, the magnitude of the free Gibbs energy (ΔG°) is obtained from the Gibbs–Helmholtz eqn (8).

$$\Delta G^\circ = \Delta H^\circ - T\Delta S^\circ \quad (8)$$

Here, ΔH° represents the standard enthalpy change, and ΔS° represents the standard entropy change. These values can be estimated using the van't Hoff eqn (9).

$$\ln K_d = \frac{\Delta S^\circ}{R} - \frac{\Delta H^\circ}{RT} \quad (9)$$

where R is the ideal gas constant, T is the absolute temperature, and K_d is the equilibrium constant, which can be described by the eqn (10).

$$K_d = \frac{Q_e}{C_e} \quad (10)$$

where Q_e is the equilibrium adsorption capacity and C_e is the equilibrium concentration.

2.4. Practical relevance and emerging trends in adsorption modeling

Although classical isotherm, kinetic, and thermodynamic models provide fundamental insights into adsorption processes, their direct application to real wastewater systems remains limited.[144,145] Most of these models are developed under controlled laboratory conditions with single-solute systems, whereas industrial effluents typically contain complex mixtures of heavy metals, dyes, and organic pollutants. Addressing such complexity requires the use of advanced approaches, including multi-component isotherms (*e.g.*, extended Langmuir and competitive Freundlich) that better describe adsorption in mixed-pollutant environments. Beyond the conventional Langmuir and Freundlich models, hybrid and extended models such as the Sips isotherm (a combination of Langmuir and Freundlich), the Redlich–Peterson isotherm (bridging homogeneous and heterogeneous adsorption behavior), and the Dubinin–Astakhov isotherm (suitable for pore-filling processes) are increasingly applied to biopolymer-based adsorbents. These models generally offer more accurate descriptions of heterogeneous surfaces and varying concentration ranges. Similarly, while the pseudo-first-order and pseudo-second-order kinetic models are widely employed, additional models such as the Elovich equation (appropriate for chemisorption on heterogeneous surfaces) and the intraparticle diffusion model (used to distinguish surface-controlled from diffusion-controlled mechanisms) are essential for deeper kinetic interpretation. Such models enable the identification of true rate-limiting steps, which is critical for reliable process scale-up. Thermodynamic analyses should go beyond simply reporting the spontaneity and feasibility of adsorption through ΔG°, ΔH°, and ΔS°. These parameters should be correlated with structural and spectroscopic characterization techniques such as FTIR, XPS, and BET surface area analysis, thereby establishing direct links between thermodynamic behavior and adsorption mechanisms like ion exchange, hydrogen bonding, or surface complexation. Emerging research trends also emphasize the integration of computational simulations, such as density functional theory (DFT) and molecular dynamics (MD), with classical adsorption models. These simulations provide atomistic-level insights into adsorption sites, binding energies, and pollutant–adsorbent interactions, thereby enhancing predictive capability. Overall, future adsorption studies should move beyond empirical model fitting. A more holistic approach that combines multi-component equilibrium models, detailed kinetic analyses, thermodynamic evaluations, and molecular-level simulations will significantly improve the reliability and practical applicability of adsorption research for real wastewater treatment scenarios.

3. Natural polymers as bioadsorbents

The term 'natural biopolymers' is used for biomolecules and polymeric materials that occur naturally and are mostly formed by living organisms during their life cycle.[146,147] The use of biopolymer-based materials for the treatment of water pollutants is a highly promising approach. This is due to the fact that bioadsorbents are often inexpensive, environmentally friendly, highly effective, and offer good regeneration opportunities.[148] Consequently, the emergence of novel challenges in the realm of developing alternative natural biopolymer-based adsorbents has unveiled pathways for researchers to eliminate toxic pollutants from water treatments.[1] In this regard, cellulose, chitosan, gelatin, alginate, starch, and carrageenan represent the most widely studied and developed natural biopolymers, with decades of research and development focused on their application in wastewater treatment.[134,149–151] These biopolymers, featuring a variety of functional groups (such as amino, hydroxyl, carboxyl, carbonyl, thiol, sulfate, *etc.*), are the primary components of bioadsorbents, playing a key role in the substantial interaction between adsorbents and pollutants (adsorbates).[152,153] These types of interactions typically occur through complexation, chelation, ion exchange, electrostatic interactions, aggregation, microprecipitation, oxidation, or reduction during the adsorption process (Fig. 3).[154–158] In this review, our primary objectives are to deliberate on a plethora of naturally occurring biopolymer-based materials as super adsorbents and to provide a synopsis of their potential application for the elimination of assorted wastewater contaminants.

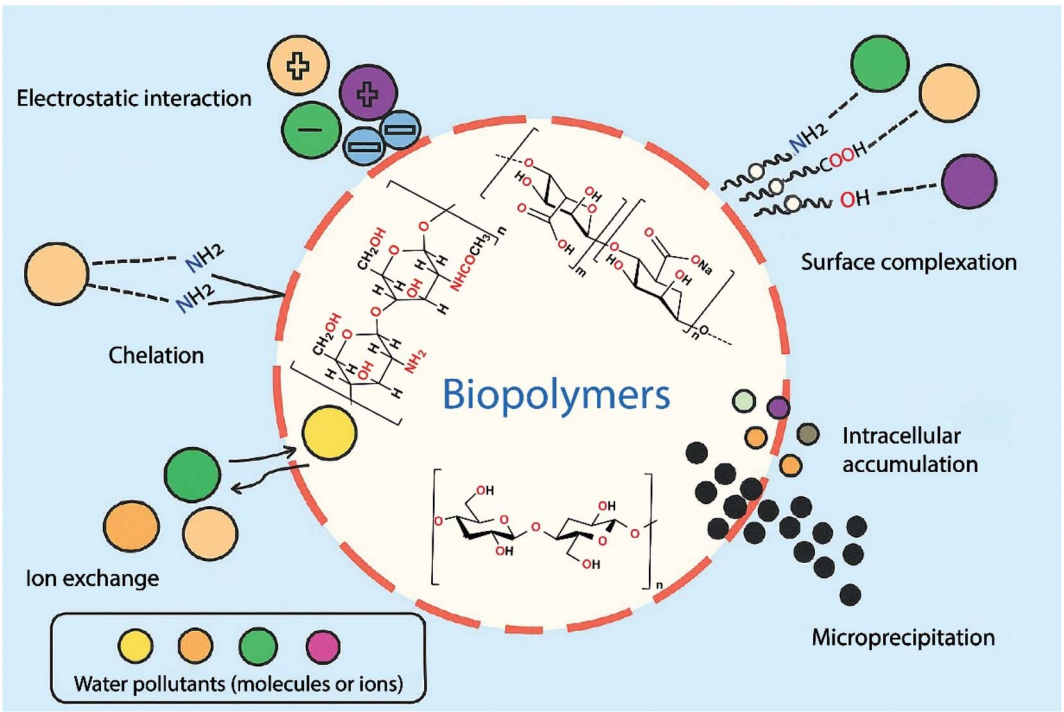

Fig. 3 Various interactions take place during the adsorption process.

3.1. Cellulose-based bioadsorbents

Cellulose is a polysaccharide with the chemical formula $(C_6H_{10}O_5)_n$, a natural biopolymer made up of a straight chain of anhydroglucose units connected through β(C1 → C4) positions.[159] It is the most abundant natural raw material among the naturally occurring polymers. Plants are the most abundant source of cellulose, which is found in various parts such as wood, cotton, and agricultural residues.[160] However, it has been observed that natural cellulose has a lower adsorption capacity than modified/functionalized cellulose.[161] Therefore, in order to enhance its adsorptive properties, the compact and inactive molecular structure of cellulose must undergo modification or functionalization. In the past decade, the establishment of a wide range of possible modifications or functionalizations of natural cellulose by researchers has occurred, along with the disclosure of several exciting findings. Cellulose-based bioadsorbents have several favorable features, including natural availability, cost-effectiveness, nontoxicity, a high specific surface area, micro/nano-size, physicochemical stability, biocompatibility and biodegradability.[162] As a result, cellulose-based bioadsorbents have been shown to be effective for

Table 2 Cellulose-based bioadsorbents towards hazardous pollutants

Cellulose-based bioadsorbents	Adsorbate (hazardous pollutants)		Adsorption capacity (mg g^{-1})	Ref.
EFB-NCP	Pb(II)	Metal ions	24.94	164
ZIF-8@CA	Cr(VI)		41.84	165
Cellulose-*graft*-poly (acrylic acid)	Cu^{2+}, Mn^{2+}		201, 175	166
In situ TEMPO functionalized nanocellulose-based membranes	Cu^{2+}, Fe^{2+}/Fe^{3+}		374, 456	167
PCA@AC	Cr(VI)		507.61	168
NCNB	Cr, Co, Cu		2749.68, 916.65, 1937.49	169
Cellulose-based porous spherical/cotton	Cu^{2+}		110	170
Magnetic chitosan/cellulose	Cu^{2+}, Pb^{2+}, Cd^{2+}		88.21, 61.12, 45.86	171
Magnetic TZFNC	Pb(II)		554.4	172
CCN–Fe_3O_4	Pb(II)		49.61	173
LCMA@PDA@PEI	Pb(II)		101.71	174
CGD	MG, BF	Dyes	458.72, 1155.76	163
Cellulose citrate (CC)	MB		96.2	175
Cellulose/chitosan aerogels (CE/CS)	CR		381.7 (303 K), 580.8 (323 K)	176
Cellulose acetate/chitosan blend films	Orange 7, brilliant yellow		9.98, 9.38	177
LCMA@PDA@PEI	MB		187.3	174
Cellulose/biochar cryogels	Petroleum, SAE20W50 oil	Others	73, 54	178

eliminating a broad range of water pollutants, such as heavy metal ions, dyes, petroleum remnants, and pesticides.[163] This section summarizes the development and use of functionalized cellulose-based biomaterials as examples of super adsorbents. Table 2 shows the adsorption capacity of several reported functionalized cellulose-based bioadsorbents toward hazardous pollutants.

The use of natural cellulose as a cost-effective precursor for the fabrication of activated carbon has been widespread. This activated carbon has a surface area of up to 1300 $m^2\ g^{-1}$ and large pore volumes – facilitating higher adsorption capacities for wastewater treatment.[161] For a similar perspective, Suhas *et al.* developed a promising approach to functionalize nanocellulose (EFB-NCP) using activated carbon obtained from empty oil palm fruit bunches that were then modified.[161] The modified nanocellulose-based bioadsorbent showed an outstanding performance toward selective removal of Pb(II), achieving 86% efficiency and a maximum adsorption capacity of 24.94 mg g^{-1}. Whereas, Yao and coworkers developed a facile method for hybrid cellulose aerogels/zeolitic imidazolate framework (termed as ZIF-8@CA) by combining organic cellulose aerogels and inorganic ZIF-8 particles to eliminate heavy metal ions from wastewater.[179] The absorption capability of the porous hybrid ZIF-8@CA for Cr(VI) was considerably enhanced, and the maximum absorption capacity (using the Langmuir isotherm model) increased up to 41.84 mg g^{-1}. The adsorption experiments yielded results showing a significant improvement in the adsorption capacity of ZIF-8@CA for Cr(VI) ions compared to cellulose-based aerogels or ZIF-8. Wang *et al.* synthesized microporous cellulose-*graft*-poly(acrylic acid) spheres as efficient adsorbents for Cu^{2+} and Mn^{2+} metal ions. The resulting biopolymers, based on cellulose and acrylic acid, showed maximum adsorption capacities of 201 mg g^{-1} and 175 mg g^{-1} for Cu^{2+} and Mn^{2+} ions, respectively.[166] Conversely, Mathew and coworkers fabricated distinctive nanocellulose-based membranes by modifying the composition of sludge microfibers/cellulose nanofibers and implementing *in situ* TEMPO surface modification to augment the removal efficiencies for heavy metal ions.[167] The *in situ* TEMPO-functionalized nanocellulose-based membranes exhibited high mechanical stability and water permeability, as well as an adsorption capacity of up to 374 mg g^{-1} for Cu^{2+} and 456 mg g^{-1} for Fe^{2+}/Fe^{3+} ions. These values were around 1.2–1.3 times higher than those of unfunctionalized cellulose nanofibers and cellulose nanocrystals. A cellulose-based composite (PCA@AC) was fabricated by adhering a catechol-amine polymer (a copolymer of catechol, tetraethylenepentamine, and *p*-phenylenediamine) onto a cellulose substrate.[168] The resulting biocomposite demonstrated a notable performance for capturing Cr(VI) ions with a capacity of 507.61 mg g^{-1}, calculated from the Langmuir isotherm model at 30 °C. The obtained value was also found to be greater than that of the pure cellulose substrate. This phenomenon is attributed to the electrostatic interaction and the reduction of Cr(VI) to Cr(III) ions during the adsorption experiments. The potential application of nanobentonite-incorporated nanocellulose/chitosan aerogel (NCNB) for removing metals from simulated wastewater was also demonstrated by Narayanasamy and coworkers.[169] The maximum adsorption capacities of NCNB were found to be 2749.685, 916.65 and 1937.49 mg g^{-1} for Cr, Co and Cu, respectively. Under the optimum conditions, the corresponding removal efficiencies were obtained as 98.90, 97.45 and 99.01% under the optimum conditions. Subsequently, Wittmar *et al.* pioneered a method for synthesizing cellulose-based porous spherical adsorbers, employing natural cotton as precursor.[180] The resulting natural bioadsorbers exhibited a maximum adsorption capacity of 110 mg per g Cu^{2+} ions.

From an economic vantage point, magnetic adsorbents have proven advantageous due to their ability to recover applied adsorbent materials from aqueous media without the necessity of filtration or centrifugation.[181,182] In this respect, a novel category of effective reusable cellulose-based magnetic bioadsorbents for water purification has garnered significant attention in recent years. The benefits of this method are that the bioadsorbents, which have been modified for a specific function, can be separated from the liquid environment using an external magnetic field, and can also be reused for the subsequent cycle after being treated with acid. The demonstrative illustrations are amino-functionalized magnetic cellulose composite,[183] porous magnetic cellulose beads,[184] magnetic carboxylated cellulose nanocrystal-based composite (CCN–Fe_3O_4). Ouyang and coworkers demonstrated the synthesis of a magnetic carboxylated cellulose nanocrystal composite (CCN–Fe_3O_4), which consists of Fe_3O_4 nanoparticles on carboxylated cellulose nanocrystals (CCN), using a co-precipitation method (Fig. 4a).[173] A comparison of the adsorption capacities of Pb(II) by Fe_3O_4, CCN, and CCN–Fe_3O_4 was conducted. The results showed that CCN–Fe_3O_4 had an adsorption capacity of 49.61 mg g^{-1}, which was higher than the capacity of CCN (25.48 mg g^{-1}) and Fe_3O_4 (15.59 mg g^{-1}) (Fig. 4b). As shown in Fig. 4c, a representative illustration of the adsorption of Pb(II) ions by magnetic CCN–Fe_3O_4 is presented, and the ions can be readily collected by applying an external magnetic force. The applied bioadsorbent can subsequently be regenerated by treating it with dilute acid. However, the adsorption capacity of the CCN–Fe_3O_4 was found to be reduced slowly after several cycles were used (Fig. 4d). Nonetheless, the performance of the bioadsorbent was quite good, with a removal ratio of more than 80% being achieved. The same strategy was used to prepare cost-effective magnetic chitosan/cellulose microspheres as an effective, recyclable adsorbent from a polymeric blend of chitosan and cellulose. The microspheres were evaluated for their ability to remove heavy metal ions (Cu^{2+}, Pb^{2+}, and Cd^{2+}).[171] Additionally, a novel magnetic thiourea-modified ZnO/nanocellulose composite (TZFNC) was developed by Alipour *et al.*, exhibiting high adsorption capacity and removal efficiency for Pb(II) ions.[172] The experimental studies yielded findings on the removal efficiency of Pb(II) ions, with a result showing 99.99% removal efficiency. The study's parameters included an adsorbent amount of 40 mg, a Pb(II) concentration of 60 mg L^{-1}, a pH of 6.5, and a contact time of 14.5 minutes. The potential of the designed bioadsorbent (TZFNC) for removing Pb(II) ions was demonstrated by its ease of magnetic separation and its ability to be recycled.

The removal of toxic dye molecules from water has also involved the use of cellulose-based bioadsorbents. For example, Zhou *et al.* reported on a cost-effective, cellulose-based bioadsorbent (CGD) that was derived from natural cellulose and modified with glycidyl methacrylate and diethylenetriamine pentaacetic acid. This bioadsorbent is used to adsorb cationic dyes, such as malachite green (MG) and basic fuchsine (BF).[163] The dye adsorption studies indicated that the adsorption (CGD) for malachite green exhibited a strong congruence with the Langmuir isotherm model, while for basic fuchsine, a congruence was observed with the Freundlich isotherm model. The calculated adsorption capacities were 1155.76 mg g^{-1} for BF and 458.72 mg g^{-1} for MG at an internal concentration of 2000 mg L^{-1}. Intriguingly, the experiments conducted to assess the recyclability exhibited that CGD retained its adsorption efficiency at approximately 85% and 90% for BF and MG dye, respectively, after four or five cycles. Later, the development of cellulose citrate (CC) as a reusable bioadsorbent by De Nino and coworkers was achieved *via* a green and convenient reaction of two natural products, cellulose and citric acid.[175] The produced cellulose citrate (CC) exhibited notable effectiveness in removing cationic methylene blue (MB) from polluted water, owing to the considerable interaction between the carboxylic groups of cellulose citrate and the cationic dye molecules. The study of adsorption revealed that the maximum capacity for MB adsorption was 96.2 mg g^{-1}. The adsorption process was found to be monolayer adsorption, indicating the Langmuir model, while for the adsorption kinetics, the pseudo-second-order model was observed.

Cellulose-based bioadsorbents have also been found to be efficient adsorbents of anionic dyes for similar purposes. For instance, Liu *et al.* prepared eco-friendly cellulose/chitosan (CE/CS) porous aerogels using sol–gel and freeze-drying techniques, varying the CE/CS mass ratio.[185] The CE/CS composite exhibited remarkable adsorption capacity for anionic Congo red (CR), with capacities of 381.7 and 580.8 mg g^{-1} at 303 and 323 K, respectively. The increase in adsorption capacity at higher temperatures clearly indicates that CR dye adsorption is an endothermic process involving electrostatic interactions and hydrogen bonding. The CE/CS aerogel exhibited enhanced removal efficiency of CR under optimal conditions, with a composite ratio of 1 : 3, an optimal adsorbent dosage of 2.5 g

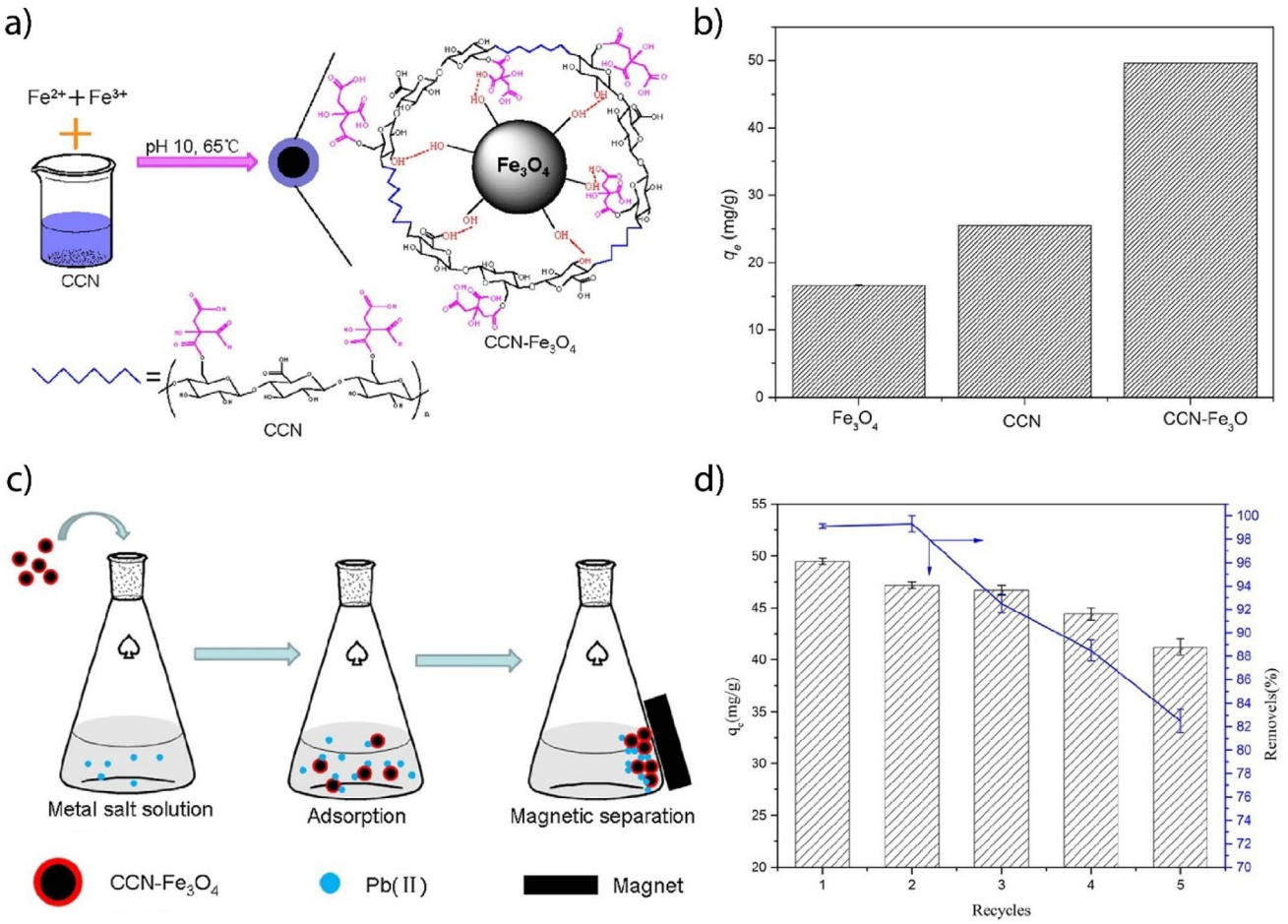

Fig. 4 (a) Scheme of the synthesis of the magnetic carboxylated cellulose nanocrystal composite (CCN–Fe_3O_4). (b) A comparison of the adsorption capacities of Pb(II) by Fe_3O_4, CCN, and CCN–Fe_3O_4. (c) Illustration of the adsorption process by a reusable magnetic CCN–Fe_3O_4 composite for the adsorption of Pb(II) ions. (d) Recyclability Adsorption Studies for Pb(II) onto CCN–Fe_3O_4 [reproduced from ref. 173 with permission from Elsevier, Copyright 2016].

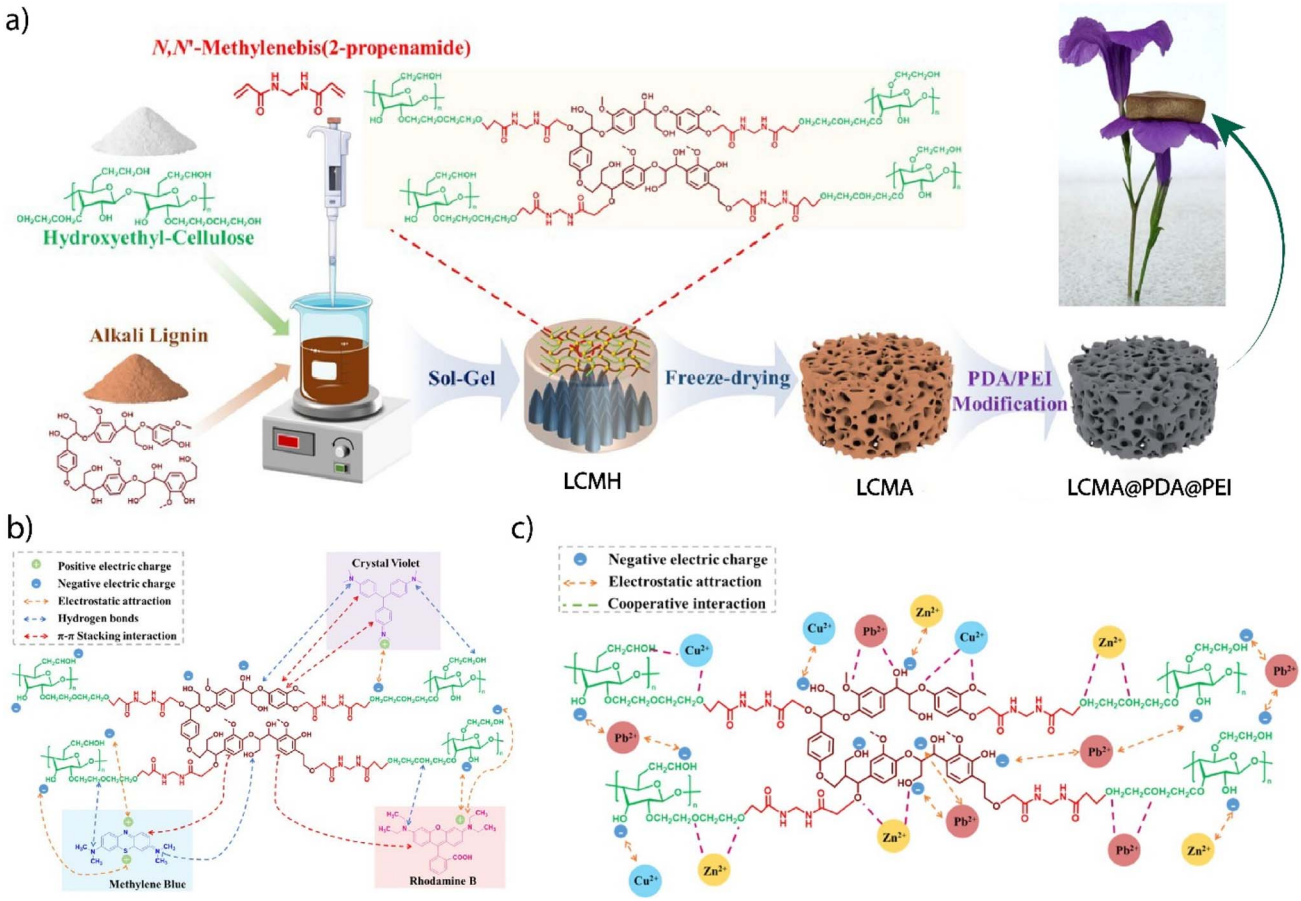

Fig. 5 (a) Scheme of the fabrication of lignin/cellulose foam absorbent (LCMA) and modification of LCMA with polydopamine (PDA) and polyethyleneimine (PEI). (b) Adsorption mechanism of LCMA on different dye molecules. (c) Adsorption mechanism of LCMA on different metal ions [reproduced from ref. 174 with permission from Elsevier, Copyright 2025].

L^{-1}, and a pH range of 3 to 11. Furthermore, Thomas and coworkers produced cellulose acetate/chitosan blend films using a practical solvent casting procedure and subsequently altered the resulting films through a deacetylation technique.[186] In this work an investigation was conducted into the adsorption behavior of cellulose acetate/chitosan composite films, both unmodified and modified, in the presence of anionic dyes, including acid orange 7 and brilliant yellow. The experimental findings demonstrated that modified cellulose acetate/chitosan composite films exhibited enhanced adsorption capacity and dye removal efficiency, with values of 9.98 mg g^{-1} and 99.8% for acid orange 7, and 9.38 mg g^{-1} and 99.7% for brilliant yellow. Whereas, Kunz Lazzari *et al.* prepared cellulose/biochar cryogels using freeze-drying techniques from *Pinus elliotti* cellulose and biochar, and studied the adsorption behavior toward organic liquids such as petroleum and SAE20W50 oil, through adsorption isotherm and kinetic models.[178] The as-synthesized cellulose/biochar cryogels showed their potential as promising bioadsorbents for petroleum and SAE20W50 oil, exhibiting high heterogeneous sorption capacities of 73 g g^{-1} and 54 g g^{-1}, respectively.

Recently, Zheng and coworkers synthesized lignin/cellulose foam adsorbents (LCMA) and investigated their adsorption mechanism for removing cationic dyes and heavy metals from wastewater.[174] A high-strength LCMA was prepared using the sol–gel method to crosslink cellulose with lignin as the skeleton (Fig. 5a). LCMA exhibited an exceptional absorption and removal capacity for cationic dyes (such as methylene blue, crystal violet and rhodamine) and heavy metal ions (*e.g.*, Cu^{2+}, Pb^{2+} and Zn^{2+}), with separation efficiencies reaching over 99.76% for cationic dyes and 99.85% for heavy metal ions. The process of adsorption by LCMA involved several synergistic mechanisms that allow efficient removal of cationic dyes and heavy metal ions from wastewater (Fig. 5b and c). Initially, electrostatic attraction occurs between the negatively charged functional groups in lignin and cellulose and the positively charged pollutants. This is followed by hydrogen bonding, supported by hydroxyl (–OH) groups in the LCMA that help stabilize the adsorbed pollutants. Aromatic units in lignin also contribute through π–π stacking interactions with dye molecules, enhancing adsorption strength. For heavy metals, complexation is significant—metal ions bond with oxygen-containing groups such as carboxyl (–COOH) and hydroxyl. Additionally, the porous structure of LCMA foam supports size exclusion by physically trapping larger pollutant particles. These combined mechanisms allow LCMA to achieve efficient

Table 3 Chitosan-based bioadsorbents towards hazardous pollutants

Chitosan-based bioadsorbents	Adsorbate (hazardous pollutants)		Adsorption capacity (mg g^{-1})	Ref.
CS-PDA	Cr(VI), Pb(II)	Metal ions	374.4, 441.2	187
Chitosan/CDTA/GO	Cr(VI)		166.98	188
Fe_3O_4@Zr–chitosan	Cr(VI)		280.97	189
Chitosan/sepiolite composite	MB, RO16	Dyes	40.98, 190.96	190
Chitosan-grafted-polyethyleneimine	Reactive black 5		707.27	191
Chitosan–$Fe(OH)_3$	MO, CR		314.45, 445.32	192
Chitosan/PVA	Nitrate ions	Acid radicals	35.03	193
Chitosan/PEG	Nitrate ions		50.68	193

and reliable performance in wastewater treatment. The super-hydrophilicity of the foams was imparted through further modification of LCMA by a facile method using polydopamine (PDA) and polyethyleneimine (PEI) (Fig. 5a). The resulting LCMA@PDA@PEI demonstrated impressive performance in separating immiscible oil–water mixtures and oil-in-water emulsions (with separation efficiencies of >99.95% and >99.05%, respectively).

3.2. Chitosan-based bioadsorbents

As the biodegradable natural polymers play a pivotal role in a myriad of applications, among them, chitosan emerges as the most promising candidate for super-adsorbents in wastewater treatment. Chitosan is another polysaccharide that is produced through the deacetylation of chitin, which is the second most prevalent natural biopolymer after cellulose. It is primarily obtained from insect cuticles and sea crustacean shells. Nevertheless, chitosan possesses various encouraging properties, such as being non-toxic, inexpensive, biodegradable, and abundant in active functional sites. However, it cannot be utilized directly for adsorption purposes due to its substandard mechanical strength, high crystallinity, limited surface area, and solubility in an acidic medium. Therefore, chitosan must be functionalized or modified for use as a potential adsorbent. It has frequently been modified into various forms, including nanofibers, composites, films, foams, blends, and hydrogel beads. Chitosan has a special chemical structure that makes it better than other polysaccharides (like cellulose or starch), rendering it highly adaptable for specific applications in the field of biology. Chitosan and its derivatives are the focus of extensive research due to their remarkable adsorption capabilities, which can be attributed to the presence of amine (or protonated NH_3^+) and hydroxyl (–OH) groups within their molecular structures. Moreover, the distinctive characteristic of chitosan's polycationic nature endows it with the capacity to function as a flocculating agent. This property enables its ability to interact with metal and organic molecules through chelation, thereby adsorbing them *via* substantial electrostatic interactions. To date, the modification of raw chitosan has been achieved through several studies involving crosslinking with other precursors, incorporating it with porous materials/polymers, and introducing functional groups through grafting. Table 3 summarizes a few examples of chitosan/chitin-based biopolymers as super adsorbents.

Hameed and coworkers prepared cross-linked chitosan/sepiolite composites using low-cost, environmentally friendly materials such as chitosan and sepiolite clay, and crosslinking process was achieved using epichlorohydrin as an additive.[190] The synthesized composite of chitosan and sepiolite was investigated as a prospective bioadsorbent for toxic dyes such as methylene blue (MB) and reactive orange 16 (RO16). The respective monolayer adsorption capacities were found to be 40.98 and 190.96 mg g^{-1} at 30 °C. The adsorption properties of chitosan can be enhanced by blending it with other polymers. For instance, Rajeswari *et al.* fabricated composites of chitosan/PVA and chitosan/PEG and investigated the adsorption of nitrate ions from water solutions.[194] The adsorption capacities of nitrate ions were found to be 35.03 mg g^{-1} for chitosan/PVA and 50.68 mg g^{-1} for chitosan/PEG. The dye adsorption capacity of chitosan was enhanced through grafting with other polymers. For instance, the adsorption capacity of the chitosan-grafted-polyethyleneimine for reactive black 5 (RB5) was reported as 707.27 mg g^{-1}, while in the case of non-grafted chitosan, it was only 209.90 mg g^{-1}.[191] Meanwhile, Zhou and coworkers fabricated chitosan–$Fe(OH)_3$ beads as efficient adsorbents for eliminating anionic dyes from contaminated water.[192] Chitosan–$Fe(OH)_3$ beads were fabricated by dissolving chitosan powder in an aqueous solution of ferric chloride ($FeCl_3$) at ambient conditions (Fig. 6a). The removal efficiency of anionic dyes, such as Congo red (CR) and methyl orange (MO), using chitosan–$Fe(OH)_3$ beads was higher than that using pure chitosan beads (Fig. 6b and c). The maximum adsorption capacities were ascertained through the implementation of the Langmuir isotherm equation, yielding values of 314.45 and 445.32 mg g^{-1} for CR and MO, respectively. The high adsorption capacity of CS–$Fe(OH)_3$ for ionic dyes (like CR and MO) was attributed to both chemical and physical mechanisms (Fig. 6d). Chemically, at pH 3, protonated amino groups on chitosan attract negatively charged dyes *via* electrostatic interactions, while $Fe(OH)_3$ enables dye binding through complexation and hydrogen bonding. Additionally, studies on the recyclability of the CS–$Fe(OH)_3$ beads indicated that the chitosan–$Fe(OH)_3$ combination was reusable and exhibited removal efficiencies for dyes of up to 95%, even after five cycles of use.

Guo *et al.* fabricated polydopamine-modified chitosan aerogels (CS–PDA) through dopamine self-polymerization and glutaraldehyde crosslinking reactions to enhance the adsorption properties and acid resistance of chitosan (Fig. 7a).[187] The

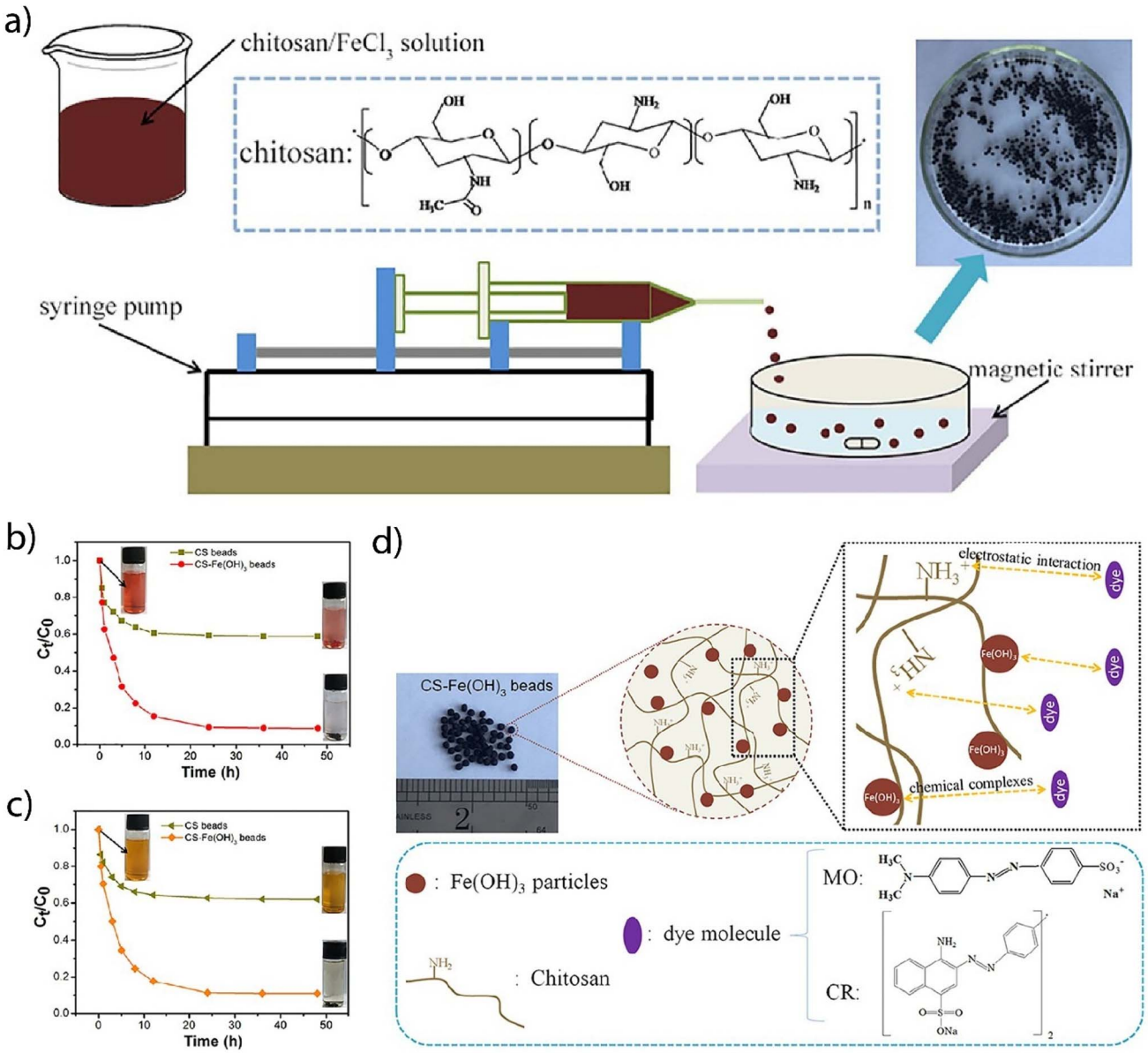

Fig. 6 (a) Scheme of the synthesis of the chitosan–$Fe(OH)_3$ beads. (b and c) The removal of Congo red (CR) and methyl orange (MO) dyes using chitosan (CS) and CS–$Fe(OH)_3$ beads. (d) Adsorption mechanism for the dye adsorption on the chitosan–$Fe(OH)_3$ beads [reproduced from ref. 195 with permission from Elsevier, Copyright 2018].

CS–PDA aerogels exhibited excellent adsorption capabilities, with maximum capacities of 374.4 and 441.2 mg g^{-1} for the removal of Cr(VI) and Pb(II) metal ions, respectively. Metal adsorption studies of the resulting CS–PDA aerogels indicated that the adsorption isotherms and kinetic data were consistent with the Langmuir isotherm and pseudo-second-order kinetic models (Fig. 7b–d). Additionally, the Thomas and Adams–Bohart models were applied to analyze and simulate the breakthrough curve (Fig. 7e). Column adsorption experiments showed that CS–PDA is effective for continuous Cr(VI) removal. Lower flow rates improved adsorption performance by increasing contact time (EBCT), allowing Cr(VI) to better interact with the adsorbent. In contrast, higher flow rates reduced removal efficiency due to insufficient residence time. Thus, slower flow rates are more favorable for effective Cr(VI) adsorption in industrial applications. The impact of coexisting ions on metal ion adsorption was systematically investigated to assess the selectivity and performance of the adsorbent in real wastewater conditions. Ali and coworkers prepared a unique chitosan-based bioadsorbent termed chitosan/CDTA/GO (chitosan/1,2-cyclohexylenedinitrilotetraacetic acid/graphene oxide) using glutaraldehyde as a cross-linker.[188] The removal efficiency of the synthesized chitosan/CDTA/GO nanoparticles toward Cr(VI) ions was evaluated under various adsorption conditions, including adsorbent dose, chemical composition of the adsorbent (CDTA/GO concentration), temperature, contact

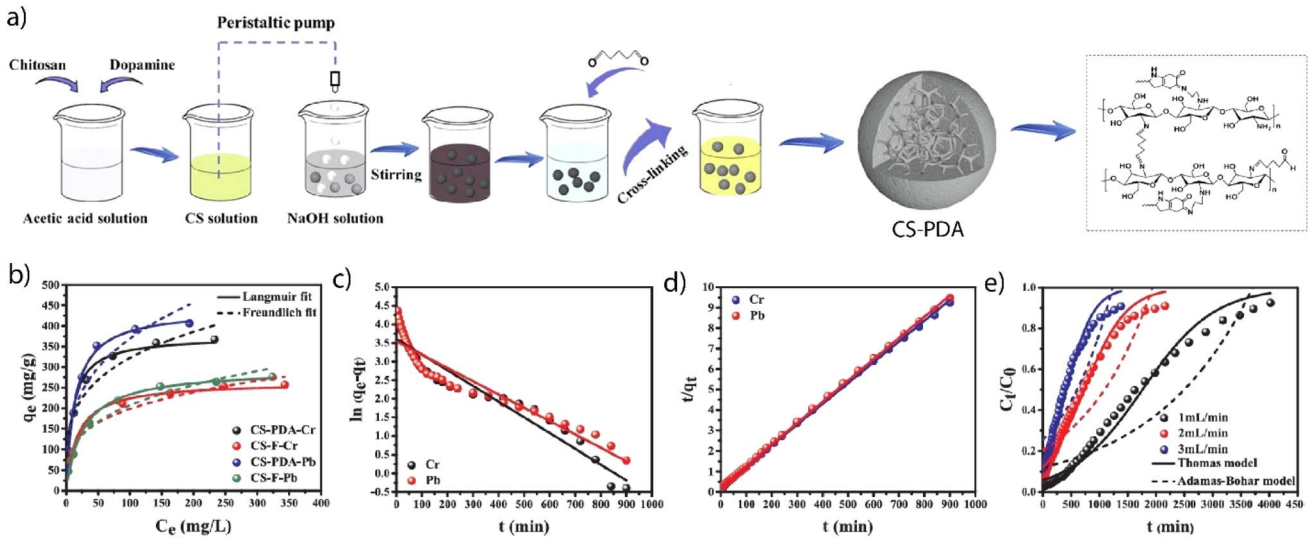

Fig. 7 (a) Scheme of the preparation of the polydopamine-modified chitosan (CS–PDA) aerogels. (b) Adsorption isotherms of Cr(VI) and Pb(II) on pure chitosan (CS–F) and CS–PDA obtained from Langmuir and Freundlich models. Fitting of the pseudo-first-order (c) and pseudo-second-order (d) kinetics models. (e) Breakthrough curves of Cr(VI) adsorption on CS–PDA at different flow rates (Thomas and Adams–Bohart models) [reproduced from ref. 187 with permission from Elsevier, Copyright 2018].

time, solution pH, and initial Cr(VI) metal ion concentration. The adsorption data revealed that the adsorption capacity of the chitosan/CDTA/GO nanoparticles toward Cr(VI) ions was 166.98 mg g^{-1} at an optimal adsorbent dose of 2 g L^{-1}, an equilibrium time of 60 minutes, and a pH value of 3.5. Additionally, the results indicated that temperature and pH can greatly affect the adsorption capacity. The adsorption processes were examined using the pseudo-second-order kinetic model, and the adsorption isotherm was analyzed using the Langmuir model.

From the perspective of ease of reuse, Chen *et al.* synthesized magnetic zirconium(IV)-crosslinked chitosan (Fe_3O_4@Zr–chitosan) microspheres as reusable bioadsorbents. These bioadsorbents were produced through a coordination reaction between the chitosan biopolymer matrix and zirconium oxychloride, and were used for effective removal and simultaneous detoxification of Cr(VI) ions in an aqueous medium.[189] The synthesized Fe_3O_4@Zr–chitosan bioadsorbent exhibited selective adsorption of Cr(VI) ions in the presence of other ions, including Na^+, K^+, Ca^{2+}, Mg^{2+}, Cu^{2+}, Zn^{2+}, Cl^-, SO_4^{2-}, CO_3^{2-}, and NO_3^-. In the batch adsorption studies of Cr(VI) ions, it was shown that the adsorption capacity of the synthesized Fe_3O_4@Zr–chitosan microspheres was found to be 280.97 mg g^{-1} at a pH of 4.0 and a temperature of 298 K. Notably, the bioadsorbent exhibited remarkable reusability for water purification, achieving a substantial reduction in effluent Cr(VI) metal ions to the ppb (parts per billion) level, thereby meeting the WHO (World Health Organization) drinking water standard.

3.3. Alginate-based bioadsorbents

Alginates are natural polysaccharides that are primarily extracted from the cell walls of brown algae through acidification and sodium salt extraction. Sodium alginate (SA) is a renewable anionic biopolymer consisting of a natural polysaccharide and α-1,4-L-glucuronic acid. It is a low-cost, water-soluble biomaterial that contains an abundance of hydroxyl (–OH) and carboxyl (–COOH) functional groups, which have a high affinity for heavy metal ions. However, sodium alginate has moderately low stability, heat resistance, and mechanical strength. Therefore, it

Table 4 Alginate-based bioadsorbents towards hazardous pollutants

Alginate-based bioadsorbents	Adsorbate (hazardous pollutants)		Adsorption capacity (mg g^{-1})	Ref.
Cu–PVA–SA	Cu(II)	Metal ions	79.3	196
Phosphate-embedded calcium alginate beads	Cd(II)		82.6	197
Alginate@PEI	Cr(VI)		431.6	198
Alginate-based attapulgite foams	Cu(II), Cd(II)		119.0, 160.0	199
Sodium alginate-based crosslinked beads	Pb(II)		2042	200
MPA	Cr(VI)		538.97	201
Sodium alginate-based crosslinked beads	MB	Dyes	2977	200
MPA	CR		3568	201

is commonly modified chemically or physically to be used as green bioadsorbents in wastewater remediation. Consequently, alginate-based bioadsorbents have received considerable attention for eliminating numerous pollutants from contaminated water. Recent studies have focused on improving raw alginate materials by incorporating various functional groups through grafting or crosslinking polymerization reactions for water treatment (see Table 4). To illustrate, Chen *et al.* fabricated alginate-based Cu(II)-imprinted porous films (Cu–PVA–SA) and investigated its capacity for extracting Cu(II) ions from an aqueous environment.[196] The effects of various parameters on adsorption behaviors were investigated by changing several factors: the concentration of Cu(II) in the Cu–PVA–SA, the adsorbent dosage, the pH of the solution, the ionic strength, the contact time, and the initial concentration of the Cu(II) solution. The resultant Cu–PVA–SA exhibited an adsorption capacity of 79.3 mg g^{-1} for Cu(II) ions under optimized conditions. In a related development, Wang *et al.* fabricated phosphate-embedded calcium alginate aerogel beads for the purpose of removing metal ions of Cd(II) ions, exhibiting a maximum adsorption capacity of 82.6 mg g^{-1}.[197] Whereas, Zhai and coworkers prepared a flexible core–shell/bead-like alginate@PEI biosorbent through cross-linking reaction using polyethylenimine (PEI) used as a modification reagent.[198] The adsorption capacity of the modified alginate@PEI for Cr(VI) was observed to be 431.6 mg g^{-1}, significantly higher than that of the unmodified sodium alginate (24.2 mg g^{-1}).

In an effort to curtail expenditures while enhancing the mechanical fortitude of alginate-based adsorbents, a conventional phyllosilicate such as attapulgite (ATP) was incorporated into the matrix. For example, Wang *et al.* prepared alginate-based attapulgite foams by encapsulating attapulgite (ATP) in sodium alginate using freeze drying and post-crosslinking techniques.[199] The resulting floatable, porous foam exhibited an impressive adsorption capacity of 119.0 mg g^{-1} for Cu(II) and 160.0 mg g^{-1} for Cd(II). Moreover, the resulting alginate-based bioadsorbents demonstrated notable chemical and mechanical stability, and were readily recyclable due to their ability to float on water. Shao *et al.* demonstrated an easy way to make special beads made of sodium alginate that can remove organic dyes and toxic metal ions.[200] The resulting beads exhibited an adsorption capacity of 2977 mg g^{-1} for methylene blue (MB) dye and 2042 mg g^{-1} for lead (Pb^{2+}) ion. Additionally, the alginate-based beads showed significant performance in absorbing methylene violet dye and other heavy metal ions, such as Cu^{2+}, Ni^{2+}, and Cd^{2+}. Whereas, Wang and coworkers fabricated an MXene/polyethyleneimine (PEI)-functionalized sodium alginate composite aerogel (MPA) by incorporating amino-functionalized $Ti_3C_2T_x$ and PEI into a sodium alginate aerogel matrix *via* crosslinking reactions.[201] The fabricated MPA bioadsorbents exhibited ultrahigh adsorption performance toward Congo Red (CR) dye and Cr(VI) metal ions due to the abundant active sites of the coupled PEI and MXene, which resulted in significant electrostatic attraction. The adsorption capacities observed were 3568 mg g^{-1} and 538.97 mg g^{-1} for Congo Red and Cr(VI) ions, respectively.

3.4. Starch-based bioadsorbents

Starch is another well-known naturally occurring biodegradable polymer that is found in the roots, stalks, and seeds of various plants. Owing to their low cost, easy availability, non-toxicity, biocompatibility, high surface area, and renewability, functionalized starch-based biopolymers have been utilized as super adsorbents for water remediation.[202,203] In this section, we highlight and summarize the potential applications of starch-based bioadsorbents for the remediation of various pollutants from wastewater in Table 5. For instance, Guo *et al.* synthesized crosslinked porous starch (CPS) by crosslinking native starch with epichlorohydrin, followed by hydrolysis of the crosslinked starch with α-amylase.[204] The resultant biodegradable adsorbent CPS was examined for its potential in the removal of methylene blue dye. The adsorption studies indicated that the adsorption data were well-fitted with the Langmuir model, with a capacity of 9.46 mg g^{-1}. Furthermore, the dye adsorption data showed that CPS has a greater removal efficiency than native starch or porous starch. Meanwhile, Singh *et al.* synthesized starch-functionalized iron oxide nanoparticles (SIONPs) and iron oxide nanoparticles (IONPs) and assessed their ability to adsorb Cr(VI) ions.[205] The experimental data showed that the adsorption capacity of SIONPs was much better than IONPs, with a monolayer adsorption capacity for Cr(VI) ions of 9.02 mg g^{-1}.

Additionally, the negative charge of starch effectively removes cationic dye molecules.[202,206] Pourjavadi *et al.* prepared a magnetic nanocomposite, nanoparticle@starch-*g*-poly(vinyl sulfate), which effectively absorbed cationic dye molecules, such as malachite green and methylene blue, and was highly reusable.[207] The nanoparticle@starch-*g*-poly(vinyl sulfate) demonstrated a substantial removal efficiency, with a capacity of 621 mg g^{-1} for MB and 567 mg g^{-1} for MG, which were comparable to or superior to the majority of other adsorbents. In a similar attempt, Ramin and coworkers fabricated a nanocomposite hydrogel consisting of starch-grafted poly(-acrylamide), graphene oxide, and hydroxyapatite (starch/GO/PAM) to absorb cationic methylene blue (MG) dye from wastewater.[208] Additionally, the temperature-dependent results for the MG dye suggested that adsorption occurred *via* an endothermic, feasible, and spontaneous process, and the dye adsorption kinetics followed the pseudo-second-order model. Adsorption experiments also showed that isotherm data fit well with the Langmuir isotherm model, which showed a capacity of 297 mg g^{-1} for cationic MG dye. Guo *et al.* prepared TiO_2/crosslinked carboxymethyl starch (TiO_2/CCMS) for the adsorption of golden yellow dye from an aqueous medium, achieving a maximum adsorption capacity of 208.77 mg g^{-1} at a temperature of 308 K.[209] Furthermore, Dai *et al.* synthesized a novel starch-based thermoresponsive hydrogel (HIPS/SA) using 2-hydroxy-3-isopropoxypropyl starch (HIPS) and sodium alginate (SA) for extracting Cu(II) metal ion from aqueous medium.[210] The HIPS/SA hydrogel with a porous network structure exhibited a high adsorption capacity of 25.81 mg g^{-1} for Cu(II) ion, which can be attributed to the numerous binding sites (carboxyl groups) within the hydrogel. Notably, the porous HIPS/SA

Table 5 Starch-based bioadsorbents towards hazardous pollutants

Starch-based bioadsorbents	Adsorbate (hazardous pollutants)		Adsorption capacity (mg g^{-1})	Ref.
SIONPs	Cr(VI)	Metal ions	9.02	204
HIPS/SA	Cu(II)		25.81	210
Crosslinked porous starch	MB	Dyes	9.46	204
Nanoparticle@starch-*g*-poly(vinyl sulfate)	MB, MG		621, 567	207
Starch/GO/PAM	MG		297	208
TiO_2/CCMS	Golden yellow		208.77	209
CMS-*g*-PMAA	NH_3, phenol	Others	31, 250.1	211

hydrogel exhibited high regenerative potential due to its thermoresponsive nature, which allowed for the rapid desorption of metal ions upon treatment with dilute hydrochloric acid. While Haq *et al.* also prepared a bioadsorbent, CMS-*g*-PMAA, which was grafted from carboxymethyl starch (CMS) and polymethacrylic acid (PMAA) for the adsorption of ammonia (NH_3) and phenol.[211] The performance of adsorbing NH_3 and phenol could be enhanced by the presence of abundant "O" centers in the CMS-*g*-PMAA. This enhancement is attributed to the formation of H-bonds between the ammonia/phenol molecules and the hydroxyl or carbonyl groups present on the adsorbent's surface.

3.5. Gelatin-based adsorbents

Gelatin, a high-molecular-weight polypeptide, is a natural biopolymer with a variety of characteristics, including water solubility, biodegradability, non-toxicity, an ample surface area, and low cost. Gelatin is used in various sectors, such as food, cosmetics, and biomedical applications. However, it is also used as a promising bioadsorbent to eliminate contaminants from wastewater because incorporating it into other compounds or materials creates network structures with various functional groups, such as NH_2, OH, and COOH. The variety of gelatin-based bioadsorbents developed includes composites, nanoparticles, blends, hydrogels, aerogels, sphere beads, membranes, films, and more. These gelatin-based biomaterials have proven to be effective and efficient adsorbents for removing water contaminants, especially organic dyes, oils, and toxic metal ions. This section summarizes important gelatin-based bioadsorbents and their potential applications in water remediation, including their adsorption capacity (Table 6). Hayeeye *et al.* prepared an eco-friendly and inexpensive gelatin/activated carbon (GE/AC) composite bead *via* a drip emulsification process to remove Pb^{2+} ions from aqueous solutions.[212] Adsorption studies revealed that the maximum adsorption capacity of GE/AC bioadsorbent beads for Pb^{2+} ions is 370.37 mg g^{-1}. This value is comparable to or better than that of natural zeolites and commercial ion exchange resins. Additionally, the influence of pH on adsorption was explored, revealing that maximum Pb^{2+} ion adsorption occurred at a pH of approximately 5.0, while low adsorption values were observed at a pH of 2.0. It is worth noting that adsorption studies of metal ions are mostly conducted at pH values around 6.0 and 7.0 because the surface of the adsorbents becomes positively charged at lower pH values, which prevents the adsorption of targeted metal ions.[213,214] Jing and coworkers synthesized a polyethylenimine (PEI)-grafted gelatin sponge that effectively absorbed heavy metals from wastewater. The absorption capacity of the PEI-grafted gelatin sponge for Pb^{2+} and Cd^{2+} ions was 66 mg g^{-1} and 65 mg g^{-1}, respectively, which was superior to that of the gelatin sponge (9.75 mg g^{-1} and 9.35 mg g^{-1}, respectively). The enhanced adsorption capacity was attributed to the robust interaction between the heavy metals and the adsorbents, enabling the wastewater to remain on the spongy PEI-grafted gelatin for extended periods. Whereas, Herman *et al.* prepared supercritically dried silica–gelatin hybrid mesoporous aerogels and assessed their Hg(II) removal efficiency *via* batch adsorption methods in the presence of other metal ions, such as Cu(II), Co(II), Ni(II), Cd(II), Pb(II), Ag(I), and Zn(II).[215] The Langmuir model was used to estimate the adsorption capacity of the silica–gelatin hybrid adsorbent, and it was observed to be 209 mg g^{-1} for Hg(II) at 24 wt% of gelatin content. Additionally, the silica–gelatin aerogel exhibited significant reusability with minimal loss of adsorption capacity after five cycles. Furthermore, Huang *et al.* successfully produced novel SPIONs/gel/PVA nanoparticles from superparamagnetic iron oxide nanoparticles (SPIONs), gelatin (gel), and polyvinyl alcohol (PVA) to extract Cu(II) and Zn(II) ions from polluted water.[216] The resulting SPIONs/gel/PVA materials showed the adsorption capacities of 56.051 mg g^{-1} for Cu(II) and 40.865 mg g^{-1} for Zn(II).

A variety of gelatin-based adsorbents have also been evaluated for removing toxic organic dyes. A few examples include chitosan–gelatin based hydrogels,[217] gelatin/calcium alginate nanofiber membranes,[218] gelatin–CNT–iron oxide nanocomposite beads,[219] and gelatin/HPET/chitosan nanocomposites.[220] In a similar attempt, Mohammadi and coworkers synthesized sepiolite/gelatin nanocomposites from naturally occurring sepiolite clay and gelatin for the cost-effective and efficient removal of dyes from wastewater.[221] The resulting sepiolite/gelatin nanocomposites exhibited high dye removal efficiency for cationic methylene blue (MB), with an adsorption capacity of 684.8 mg g^{-1} at an equilibrium time of 30 min. In contrast, Jiang *et al.* prepared a multifunctional gelatin/TiO_2/PEI (GTP) composite aerogel with a hierarchical porous structure, using natural gelatin, branched polyethyleneimine, and TiO_2 nanoparticles.[222] The as-synthesized gelatin/TiO_2/PEI composites showed a great potential in wastewater treatment, demonstrating combined performance in the removal of copper

Table 6 Gelatin-based bioadsorbents towards hazardous pollutants

Gelatin-based bioadsorbents	Adsorbate (hazardous pollutants)		Adsorption capacity (mg g^{-1})	Ref.
Gelatin/activated carbon composite bead	Pb(II)	Metal ions	370.37	212
PEI-grafted gelatin sponge	Pb(II), Cd(II)		66, 65	225
Silica–gelatin hybrid mesoporous aerogels	Hg(II)		209	215
SPIONs/gel/PVA nanoparticles	Cu(II), Zn(II)		56.051, 40.865	216
Sepiolite/gelatin nanocomposites	MB	Dyes	684.8	221
Gelatin/TiO_2/PEI composites	CV, MO, CR		64.31, 85.21, 86.67	222
Gelatin templated hierarchically porous calcium oxide composites	Organophosphate pesticides	Others	3895	224

(Cu) ions, adsorption of organic dyes, oil/water separation and photocatalytic properties. The aerogels, composed of gelatin, TiO_2 and PEI, demonstrated their ability to remove cationic dyes such as methylene blue (MB) and crystal violet (CV), and anionic dyes such as Congo red (CR) and methyl orange (MO). The adsorption capacity of these aerogels was observed to be 64.31, 85.21, and 86.67 mg g^{-1} for CV, MO, and CR, respectively, at an initial concentration of 500 mg L^{-1}. Moreover, the removal of organophosphate pesticides (phosmet) has been reported using gelatin-based adsorbents.[223] To illustrate, Kakkar and coworkers fabricated a gelatin-templated hierarchical porous calcium oxide composite (Hr–CaO) using precipitation technique by employing a water/glycerol solvent mixture and gelatin as a template.[224] The gelatin-based composites thus obtained exhibited a noteworthy adsorption capacity of 3895 mg g^{-1} for the organophosphate pesticides at an adsorbent dosage of 0.1 g L^{-1}.

3.6. Carrageenan-based bioadsorbents

Carrageenan is a unique class of linear sulfated polysaccharides consisting of a linear 1,3-glycosidically linked β-D-galactopyranose moiety and 1,4 glycosidic-linked 3,6-anhydro-α-D-galactopyranose or 1,4 glycosidic-linked α-D-galactopyranose units. Carrageenan has an anionic charge across its polymer backbone and can be extracted from red seaweed. The common forms of carrageenan are kappa-, lambda-, and iota-carrageenan, which are based on the degree of sulfation. These types are used to prepare polymeric nanocomposites, gels, beads, and membranes. Due to its highly negatively charged structure, carrageenan can easily attract species with a positive charge, and it is also used as an attractive bioadsorbent for removing toxic heavy metal ions and cationic dye molecules. A variety of carrageenan-based bioadsorbents have been developed in the form of composites or hybrid materials in the context of literature. Some illustrative examples are κ-carrageenan/poly(glycidyl methacrylate) composite,[226] cellulose/carrageenan/TiO_2 composite,[227] κ-carrageenan/poly(acrylic acid)/CdS hydrogel,[228] κ-carrageenan/silver composite,[229] κ-carrageenan/graphene oxide composite gel beads (κ-Car/GO GBs),[230] carrageenan/reduced GO/Ag composite,[231] lambda carrageenan/hydroxyapatite composite,[232] chitosan/κ-carrageenan magnetic composite,[233] κ-carrageenan/silica hybrid magnetic shells,[234] chitosan/kappa-carrageenan magnetic nanocomposite,[235] carrageenan/carbon nanotube composite,[236] and κ-carrageenan-*g*-poly(acrylamide)/sepiolite hydrogel.[237] This section summarizes different carrageenan-based materials as super bioadsorbents in Table 7.

For example, Doroudian and coworkers synthesized a novel aminosilica-functionalized and TiO_2-immobilized carrageenan hydrogel (κC-*g*-PAA/TiO_2–NH_2) that exhibited an exceptional adsorption capacity of 833 mg g^{-1} for the cationic malachite green (MG) dye, which can be attributed to the high specific surface area and active functionality of the hydrogel.[238] Men and coworkers synthesized a series of ecofriendly bioadsorbents, κ-Car/GO gel beads, from κ-carrageenan and graphene oxide.[230] The adsorption capacity of κ-Car/GO GBs for methylene blue

Table 7 Carrageenan-based bioadsorbents towards hazardous pollutants

Carrageenan-based bioadsorbents	Adsorbate (hazardous pollutants)		Adsorption capacity (mg g^{-1})	Ref.
κ-Carrageenan/poly(glycidyl methacrylate) composite	MB	Dyes	166.62	226
κ-Carrageenan/poly(*N*-vinylpyrrolidone-*co*-acrylic acid) composite	ST, BCB		362.5, 398	240
κ-Car/GO GBs	MB		658.4	230
κ-Carrageenan/silica magnetic shells	MB		350	234
κ-C-*g*-PAA/TiO_2–NH_2	MG		833	238
Chitosan/carrageenan/Fe_2O_3	CR, MB		190, 118	239
Agar/κ-carrageenan hydrogel	MB		242.3	242
Bio-based i-carrageenan aerogels	Cr(VI), Co(II), Mn(II), Cu(II), Cd(II)	Metal ions	105, 144.9, 133, 158.7, 128	241
Chitosan/carrageenan/Fe_2O_3	Cu(II), Cr(III)		17.9, 10.8	239

dye was observed to be 658.4 mg g^{-1}, with minimal dye removal efficiency decrease after five cycles. Whereas, Liang *et al.* prepared a chitosan/carrageenan/Fe_2O_3 magnetic composite to remove cationic and anionic dyes and heavy metal ions from wastewater.[239] The chitosan/carrageenan/Fe_2O_3 nanocomposite demonstrated excellent adsorption capabilities, with values of 190 and 118 mg g^{-1} for the removal of toxic dyes, including Congo red and methylene blue, respectively. Additionally, its adsorption capacity for metal ions such as Cu(II) and Cr(III) was found to be 17.9 and 10.8 mg g^{-1}, respectively. Choudhury *et al.* synthesized a bioadsorbent of poly(*N*-vinylpyrrolidoneco-acrylic acid)/carrageenan composite using poly(*N*-vinylpyrrolidone-*co*-acrylic acid) and κ-carrageenan.[240] The resulting carrageenan-based bioadsorbents demonstrated effective adsorption capabilities, with values of 362.5 and 398 mg g^{-1} for organic dyes such as Safranine T (ST) and brilliant cresyl blue (BCB), respectively. These results were achieved with a binary mixture of each dye solution containing 100 mg L^{-1} at an adsorbent dose of 0.25 mg L^{-1}. While, Abdellatif *et al.* prepared new bio-based iota-carrageenan magnetic aerogels by crosslinking iota-carrageenan and PAMAM (polyamidoamine hyperbranched polymer, generation 1).[241] The as-synthesized aerogel, endowed with active sites bearing –COOH, –OH (from acrylic acid) and a sulfate group (from carrageenan), exhibited an exemplary adsorption capacity for hazardous metal ions, attributable to the substantial electrostatic interaction between the adsorbent and metal ions. Furthermore, the presence of polydopamine enhanced the adsorption capacity of the terminal amine functional groups due to the formation of a coordination complex with metal ions. The carrageenan-based aerogel exhibited an adsorption capacity of 105 mg g^{-1} for Cr(VI), 144.9 mg g^{-1} for Co(II), 133 mg g^{-1} for Mn(II), 158.7 mg g^{-1} for Cu(II), and 128 mg g^{-1} for Cd(II). Duman *et al.* (2020) prepared agar/κ-carrageenan composite hydrogel *via* a free radical reaction using tri(ethylene glycol) divinyl ether as a crosslinker.[242] The agar/κ-carrageenan hydrogel was investigated for its ability to absorb methylene blue dye from an aqueous solution. The adsorption capacity was found to be 242.3 mg g^{-1} at a temperature of 35 °C and a pH of 7.

3.7. Other biopolymer-based adsorbents

In addition to these, other biopolymers, including collagen, agar, and lignin, have been explored as highly effective adsorbents for various toxic pollutants. A comprehensive overview of these materials is provided in Table 8. A naturally occurring polymer matrix consisting of amino acids is known as collagen. The hyperbranched structure of collagen is known to possess many beneficial properties, which make it a good bioadsorbent in wastewater treatment. For example, Wang *et al.* synthesized carboxylated collagen fiber (CCF) by functionalizing collagen fibers with glyoxylic acid.[243] The resulting CCF was an effective bioadsorbent for eliminating Cr(III) ions from contaminated water. The adsorption capacity toward Cr(III) ions increased by 74.13% after modification, with a maximum capacity of 106.88 mg g^{-1}. Meanwhile, Qiang *et al.* synthesized hyperbranched aminated collagen fibers by modifying collagen fibers with ethylenediamine and using cyanuric chloride as a crosslinking agent. These modified, collagen-based fibers were recognized as effective bioadsorbents for eliminating the acid black dye NT from wastewater.[244] To stabilize collagen, Thanikaivelan *et al.* fabricated collagen/iron oxide nanoparticle composites using iron oxide nanoparticles for oil-water separation. Oil adsorption studies found that the collagen-based bioadsorbent had a maximum adsorption capacity of 2 g g^{-1} for motor oil. Additionally, the magnetic properties of the iron oxide nanoparticles allowed for easy separation of the adsorbent from the aqueous medium.[245]

Agar is a hydrophilic polysaccharide composed of neutral agarose and the fraction agaropectin, which has a similar composition to starch. It is extracted from certain red algae. It is one of the oldest dynamic phycocolloids, soluble in hot water, and is primarily used to prepare solid microbiological culture media. Various agar/agarose-based bioadsorbents have been developed for water treatment applications. For instance, Li and coworkers prepared magnetic agarose-based microspheres (Fe_3O_4@agarose) to remove radionuclides from an aqueous medium.[246] The as-synthesized Fe_3O_4@agarose composite showed high adsorption capacities of 1.15 and 1.27 mmol g^{-1} for uranium (U^{6+}) and europium (Eu^{3+}) radionuclides, respectively, and could be easily separated from an aqueous medium using external magnetic forces. Patra *et al.* synthesized agar-

Table 8 Other biopolymer-based adsorbents towards hazardous pollutants

Other biopolymer-based adsorbents	Adsorbate (hazardous pollutants)		Adsorption capacity (mg g^{-1})	Ref.
Carboxylated collagen fiber	Cr(III)	Inorganic	106.88	243
Fe_3O_4@Agarose	U(VI), Eu(III)		1.15, 1.27 (mmol g^{-1})	246
Lignin-based hybrid magnetic nanoparticles	Pb(II), Cu(II)		150.33, 70.69	247
ECLNPs	Pb(II), Cu(II)		126, 54.4	248
Lignin–montmorillonite composite hydrogel	Pb(II), Cd(II), Hg(II), As(III)		11.92, 11.58, 11.85, 11.57	249
Agar@Fe/Pd	MB, RB	Organic	875, 780	250
Agarose/rGO	RB, aspirin		321.7, 196.4	251
Agar/graphene oxide aerogel	MB		578	252
Collagen/iron oxide nanoparticles	Motor oil		2 g g^{-1}	245

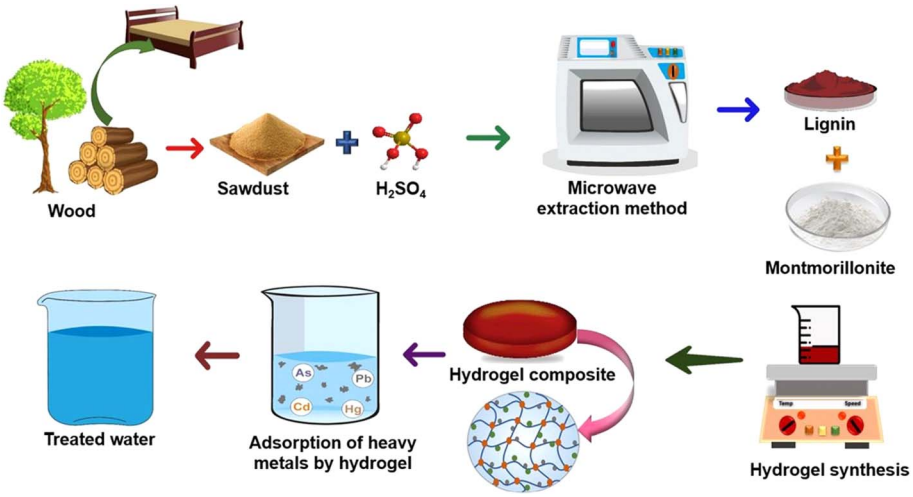

Fig. 8 A schematic overview of the preparation of a lignin–montmorillonite composite hydrogel and the adsorption of heavy metals [reproduced from ref. 249 with permission from American Chemical Society, Copyright 2024].

based hybrid bioadsorbents by altering monometallic or bimetallic nanoparticles (*e.g.*, Fe, Cu, Pd, Fe/Pd, and Fe/Cu) to eliminate toxic cationic dyes, such as methylene blue (MB) and rhodamine B (RB).[250] The agar@Fe/Pd nanoparticle aerogel demonstrated adsorption capabilities of 875 mg g^{-1} for MB and 780 mg g^{-1} for RB dye. The agar-based bioadsorbents also demonstrated in the recyclability studies were found to be reusable for over 20 cycles, exhibiting up to a 90% removal efficiency. Wang *et al.* prepared hydrophobic hydrogel beads with microchannels consisting a hybrid agarose/rGO for the selective adsorption of organic compounds from water.[251] Notably, the fabricated rGO-incorporated agarose hydrogels exhibited an exceptional capacity for water-soluble organic compounds, such as dyes and pharmaceutical drugs, attributable to the π–π interaction with the rGO. The agarose/rGO hydrogel beads exhibited remarkable adsorption capacities of 321.7 mg g^{-1} and 196.4 mg g^{-1} for RB dye and aspirin, respectively. Meanwhile, Chen *et al.* fabricated an agar/graphene oxide aerogel using a vacuum freeze-drying technique and evaluated its adsorption capacity for the methylene blue dye.[252] The Langmuir isotherm models were used to determine the adsorption capacity of agar/graphene oxide aerogel for MB dye, and it was found to be 578 mg g^{-1}.

Lignin is also a natural biopolymer that is derived from black liquor and is regarded as a low-cost bioadsorbent in comparison to activated carbon for the elimination of toxic metal ions.[140] The presence of polyhydric phenols and other active functional groups in lignin is the key factor responsible for its high adsorption capability. For instance, Fatehi and coworkers synthesized lignin-based hybrid magnetic nanoparticles as bioadsorbents using a simple method involving epichlorohydrin as a crosslinker of carboxymethylated lignin and amino-functionalized magnetic nanoparticles to eliminate heavy metal ions.[247] The resulting hybrid nanoparticles showed good adsorption capacity of 150.33 mg g^{-1} for Pb^{2+} and 70.69 mg g^{-1} for Cu^{2+} ions. The resulting hybrid nanoparticles exhibited adsorption capacities of 150.33 mg g^{-1} and 70.69 mg g^{-1} for Pb^{2+} and Cu^{2+} ions, respectively. The adsorption equilibrium for these metal ions onto the lignin-based hybrid adsorbent was achieved in 30 seconds. This equilibrium time indicates that the adsorbent could be promising for the removal of Pb^{2+} and Cu^{2+} metal ions. While Xie *et al.* synthesized modified eucalyptus lignin nanospheres (ECLNPs) and explored the adsorption ability of lead and copper metal ions for wastewater treatments.[248] The adsorption capacities of ECLNPs for Pb(II) and Cu(II) ions were found to be 126 mg g^{-1} and 54.4 mg g^{-1}, respectively. Patel and coworkers recently developed a lignin–montmorillonite hydrogel using lignin extracted from teak wood *via* microwave-assisted acidolysis (Fig. 8).[249] The trace metals (Pb(II), Cd(II), Hg(II), and As(III)) were effectively removed from water by the hydrogel, following pseudo-second-order kinetics and the Langmuir isotherm, indicating efficient monolayer adsorption. The hydrogel maintained over 50% removal efficiency after five reuse cycles in real wastewater, demonstrating its potential as a sustainable, cost-effective solution for large-scale water treatment.

4. Conclusions and future perspectives

4.1. Conclusions

This review has highlighted the transformative potential of natural biopolymer-based porous materials as next-generation adsorbents for wastewater remediation. With the escalating crisis of global water pollution, solutions must be both effective and sustainable. Biopolymers such as cellulose, chitosan, alginate, starch, and gelatin fulfil this dual role due to their renewable origin, biodegradability, low toxicity, and versatile surface chemistry. Their inherent functional groups (–OH, –NH_2, –COOH, –OSO_3^-) enable precise tailoring into composites, hydrogels, aerogels, and membranes designed for specific

pollutant removal *via* ion exchange, complexation, and hydrogen bonding.

Recent advances—including the incorporation of magnetic nanoparticles, nanoscale fillers, and hybrid materials—have overcome traditional limitations, leading to enhanced stability, adsorption capacities exceeding 99%, and easy recyclability. Collectively, these findings confirm that biopolymer-derived adsorbents offer a sustainable alternative to conventional, resource-intensive technologies and directly support the United Nations Sustainable Development Goals (SDGs), particularly SDG 6 (Clean Water), SDG 13 (Climate Action), and SDG 14 (Life Below Water).

4.2. Future perspectives and challenges

Despite impressive laboratory-scale progress, large-scale adoption remains constrained by several challenges. Key directions for future research include the following.

(1) Bridging the lab-to-industry gap: moving from batch experiments to continuous-flow, pilot-scale systems is essential. Column studies should address parameters such as hydraulic loading, bed depth, pressure drop, and long-term performance in real effluents containing competing ions and organic matter. These data are critical for techno-economic analysis and industrial acceptance.

(2) Engineering stability and selectivity: although functionalization improves adsorption, the mechanical and hydrolytic stability of biopolymers under harsh conditions (extreme pH, high salinity) is still limited. Developing robust, cross-linked networks and designing adsorbents with high selectivity for priority pollutants (*e.g.*, Pb(II), Cr(VI), pharmaceuticals) through molecular imprinting or ligand grafting will be vital for real-world applications.

(3) Sustainable regeneration and life-cycle assessment (LCA): regeneration strategies must be green, low-cost, and non-toxic, such as mild eluents, electrochemical, or biological methods. Comprehensive cradle-to-grave LCAs are urgently needed to verify the true environmental advantages of biopolymer adsorbents compared to established alternatives like activated carbon.

(4) Circular economy and waste-to-wealth approaches: using agricultural and food-industry residues (*e.g.*, crustacean shells, fruit peels, rice husks) as feedstock could lower costs and maximize sustainability. This aligns with circular economy principles and improves the economic viability of large-scale deployment.

(5) Intelligent and multifunctional systems: the next frontier lies in "smart" biopolymer composites that respond to stimuli (pH, temperature, light) for controlled adsorption and self-regeneration. Combining adsorption with catalytic degradation (*e.g.*, photocatalytic or Fenton-like processes) could achieve complete mineralization of persistent organic pollutants, offering more comprehensive remediation solutions.

In summary, natural biopolymer-based porous adsorbents stand at the forefront of sustainable water purification technologies. By uniting material innovation, green processing, and interdisciplinary collaboration, these systems can transition from laboratory research to industrial-scale applications, redefining the future of clean water treatment and contributing meaningfully to global sustainability.

Conflicts of interest

The authors declare no conflict of interest.

Data availability

No primary research results, software, or code have been included, and no new data were generated or analyzed as part of this review.

Acknowledgements

A. A. expresses gratitude to the DST INSPIRE Faculty Fellowship (IFA24-MS215) Program and the Bose Institute under the Department of Science and Technology of the Government of India for their financial support and research facilities. A. H. would like to thank IIT Patna for the research fellowship. Z. S. is thankful to the University Grants Commission (UGC) for the Junior Research Fellowship (JRF). N. D. acknowledges IIT Patna for providing research facilities.

References

1 W. Al-Gethami, M. A. Qamar, M. Shariq, A.-N. M. A. Alaghaz, A. Farhan, A. A. Areshi and M. H. Alnasir, *RSC Adv.*, 2024, **14**, 2804–2834.
2 A. Lemfarrak, A. Benzakour, M. Ouhssine and N. Benlemlih, *Ecol. Eng. Environ. Technol.*, 2025, **26**, 247–267.
3 C. C. Obijianya, E. Yakamercan, M. Karimi, S. Veluru, I. Simko, S. Eshkabilov and H. Simsek, *Water*, 2025, **17**, 2083.
4 S. Thakur, A. Sinha and A. G. Bag, *Water, Air, Soil Pollut.*, 2025, **236**, 746.
5 J. Nyika and M. O. Dinka, in *The Silent Wastewater Problem in Sub-saharan Africa*, ed. J. Nyika and M. O. Dinka, Springer Nature Switzerland, Cham, 2025, pp. 1–26, DOI: **10.1007/978-3-031-90143-0_1**.
6 A. Boretti and L. Rosa, *npj Clean Water*, 2019, **2**, 15.
7 A. E. Ercin and A. Y. Hoekstra, *Environ. Int.*, 2014, **64**, 71–82.
8 D. Bekchanov, M. Mukhamediev, S. Yarmanov, P. Lieberzeit and A. Mujahid, *Carbohydr. Polym.*, 2024, **323**, 121397.
9 S. Khademolqorani, K. J. Shah, M. Dilamian, A. I. Osman, E. Altiok, S. Azizi, I. Kamika, Y. Yang, F. Yalcinkaya, A. Yvaz and S. N. Banitaba, *Adv. Sustainable Syst.*, 2025, **6**, 2500035.
10 P. Samanta, A. V. Desai, S. Let and S. K. Ghosh, *ACS Sustain. Chem. Eng.*, 2019, **7**, 7456–7478.
11 S. Let, S. Dutta, P. Samanta, S. Sharma and S. K. Ghosh, *ACS Appl. Mater. Interfaces*, 2021, **13**, 51474–51484.
12 S. Chandra, A. Hassan, Prince, A. Alam and N. Das, *ACS Appl. Polym. Mater.*, 2022, **4**, 6630–6641.
13 A. Hassan and N. Das, *ACS Appl. Eng. Mater.*, 2024, **2**, 56–66.

14 D. S. P. Franco, J. Georgin and C. Ramprasad, in *Remediation of Heavy Metals*, 2024, pp. 1–13, DOI: 10.1002/9781119853589.ch1.
15 R. Ahmad Aftab, M. Yusuf, F. Ahmad, M. Danish, S. Zaidi, D. V. N. Vo, A.-T. Nguyen, M. M. Rahman and H. Ibrahim, *Chem.–Asian J.*, 2024, **19**, e202400154.
16 P. B. Rathod, M. P. Singh, A. S. Taware, S. U. Deshmukh, C. K. Tagad, A. Kulkarni and A. B. Kanagare, *Environ. Pollut. Bioavailability*, 2024, **36**, 2329660.
17 H. Chawla, S. K. Singh and A. K. Haritash, *Environ. Sci. Pollut. Res.*, 2024, **31**, 127–143.
18 H. U. Rahman, M. Khan and A. Ditta, *Bioremediation and Nanotechnology for Climate Change Mitigation*, ed. A. A. H. Abdel Latef, E. M. Zayed and A. A. Omar, Springer Nature Singapore, Singapore, 2025, pp. 103–136, DOI: 10.1007/978-981-96-3069-1_5.
19 K. Mohanrasu, A. C. Manivannan, H. J. R. Rengarajan, R. Kandaiah, A. Ravindran, L. Panneerselvan, T. Palanisami and C. I. Sathish, *npj Mater. Sustainability*, 2025, **3**, 13.
20 M. Sheraz, X.-F. Sun, A. Siddiqui, S. Hu and Z. Song, *Polymers*, 2025, **17**, 559.
21 S. Sinha, *Environ. Qual. Manage.*, 2024, **34**, e22320.
22 J. Guo, X. Li, Y. Feng and R. You, *Adv. Sustainable Syst.*, 2025, **9**, 2400965.
23 G. Crini and E. Lichtfouse, *Environ. Chem. Lett.*, 2019, **17**, 145–155.
24 G. Chen, *Sep. Purif. Technol.*, 2004, **38**, 11–41.
25 M. Salgot and M. Folch, *Curr. opin. Environ. Sci. Health*, 2018, **2**, 64–74.
26 R. Baby, B. Saifullah and M. Z. Hussein, *Nanoscale Res. Lett.*, 2019, **14**, 341.
27 W.-H. Chen, A. T. Hoang, S. Nižetić, A. Pandey, C. K. Cheng, R. Luque, H. C. Ong, S. Thomas and X. P. Nguyen, *Process Saf. Environ. Prot.*, 2022, **160**, 704–733.
28 A. Hassan, M. M. R. Mollah, S. Das and N. Das, *J. Mater. Chem. A*, 2023, **11**, 17226–17236.
29 F. Fu and Q. Wang, *J. Environ. Manage.*, 2011, **92**, 407–418.
30 A. Dąbrowski, Z. Hubicki, P. Podkościelny and E. Robens, *Chemosphere*, 2004, **56**, 91–106.
31 C. Zamora-Ledezma, D. Negrete-Bolagay, F. Figueroa, E. Zamora-Ledezma, M. Ni, F. Alexis and V. H. Guerrero, *Environ. Technol. Innovation*, 2021, **22**, 101504.
32 T. Robinson, G. McMullan, R. Marchant and P. Nigam, *Bioresour. Technol.*, 2001, **77**, 247–255.
33 A. Alam, A. Hassan, R. Bera and N. Das, *Mater. Adv.*, 2020, **1**, 3406–3416.
34 A. Hojjati-Najafabadi, M. Mansoorianfar, T. Liang, K. Shahin and H. Karimi-Maleh, *Sci. Total Environ.*, 2022, **824**, 153844.
35 A. Saravanan, P. Senthil Kumar, S. Jeevanantham, S. Karishma, B. Tajsabreen, P. R. Yaashikaa and B. Reshma, *Chemosphere*, 2021, **280**, 130595.
36 S. Bolisetty, M. Peydayesh and R. Mezzenga, *Chem. Soc. Rev.*, 2019, **48**, 463–487.
37 S. Ghafoori, M. Omar, N. Koutahzadeh, S. Zendehboudi, R. N. Malhas, M. Mohamed, S. Al-Zubaidi, K. Redha, F. Baraki and M. Mehrvar, *Sep. Purif. Technol.*, 2022, **289**, 120652.
38 B. L. Phoon, C. C. Ong, M. S. Mohamed Saheed, P.-L. Show, J.-S. Chang, T. C. Ling, S. S. Lam and J. C. Juan, *J. Hazard. Mater.*, 2020, **400**, 122961.
39 T. A. Kurniawan, P.-S. Yap and Z. Chen, *Environ. Chem. Lett.*, 2025, **23**, 517–577.
40 T. E. Oladimeji, M. Oyedemi, M. E. Emetere, O. Agboola, J. B. Adeoye and O. A. Odunlami, *Heliyon*, 2024, **10**, e40370.
41 A. Matilainen, M. Vepsäläinen and M. Sillanpää, *Adv. Colloid Interface Sci.*, 2010, **159**, 189–197.
42 X. Tang, H. Zheng, H. Teng, Y. Sun, J. Guo, W. Xie, Q. Yang and W. Chen, *Desalin. Water Treat.*, 2016, **57**, 1733–1748.
43 N. Zaki, N. Hadoudi, A. Charki, N. Bensitel, H. E. Ouarghi, H. Amhamdi and M. h. Ahari, *Sep. Sci. Technol.*, 2023, **58**, 2619–2630.
44 N. Ramkumar and P. Monash, *Environ. Sci.: Water Res. Technol.*, 2025, **11**, 1086–1136.
45 M. Elimelech and W. A. Phillip, *Science*, 2011, **333**, 712–717.
46 J. Shamshad and R. Ur Rehman, *Environ. Sci.: Adv.*, 2025, **4**, 189–222.
47 N. O. Etafo, D. G. Adekanmi, O. S. Awobifa, J. R. P. Torres, L. A. I. Herrera and O. A. Awobifa, *Discover Civ. Eng.*, 2025, **2**, 103.
48 H. Jiao, X. He, J. Sun, T. Elsamahy, R. Al-Tohamy, M. Kornaros and S. S. Ali, *Energy Ecol. Environ.*, 2024, **9**, 1–24.
49 R. K. Bhuvanendran, B. K. Jagadeesan, J. Karthigeyan, S. Bhuvaneshwari, S. Vallinayagam and A. S. N. Prasannakumari, *J. Mater. Cycles Waste Manage.*, 2024, **26**, 2634–2655.
50 J. Radjenovic and D. L. Sedlak, *Environ. Sci. Technol.*, 2015, **49**, 11292–11302.
51 J. R. Werber, C. O. Osuji and M. Elimelech, *Nat. Rev. Mater.*, 2016, **1**, 16018.
52 S. Jamaly, N. N. Darwish, I. Ahmed and S. W. Hasan, *Desalination*, 2014, **354**, 30–38.
53 Z. Yang, Y. Zhou, Z. Feng, X. Rui, T. Zhang and Z. Zhang, *Polymers*, 2019, **11**, 1252.
54 N. A. A. Qasem, R. H. Mohammed and D. U. Lawal, *npj Clean Water*, 2021, **4**, 36.
55 R. Zhang, Y. Liu, M. He, Y. Su, X. Zhao, M. Elimelech and Z. Jiang, *Chem. Soc. Rev.*, 2016, **45**, 5888–5924.
56 S. Verma, A. Daverey and A. Sharma, *Environ. Technol. Rev.*, 2017, **6**, 47–58.
57 A. Cescon and J.-Q. Jiang, *Water*, 2020, **12**, 3377.
58 Š. Zezulka, B. Maršálek, E. Maršálková, K. Odehnalová, M. Pavlíková and A. Lamaczová, *Processes*, 2024, **12**, 2627.
59 K. C. Khulbe and T. Matsuura, *Appl. Water Sci.*, 2018, **8**, 19.
60 R. Rashid, I. Shafiq, P. Akhter, M. J. Iqbal and M. Hussain, *Environ. Sci. Pollut. Res.*, 2021, **28**, 9050–9066.
61 Y. C. Sharma, V. Srivastava, V. K. Singh, S. N. Kaul and C. H. Weng, *Environ. Technol.*, 2009, **30**, 583–609.
62 I. Ali, M. Asim and T. A. Khan, *J. Environ. Manage.*, 2012, **113**, 170–183.
63 V. S. Tran, H. H. Ngo, W. Guo, J. Zhang, S. Liang, C. Ton-That and X. Zhang, *Bioresour. Technol.*, 2015, **182**, 353–363.

64 S. Wang, H. Sun, H. M. Ang and M. O. Tadé, *Chem. Eng. J.*, 2013, **226**, 336–347.
65 J. Wang and S. Zhuang, *Crit. Rev. Environ. Sci. Technol.*, 2017, **47**, 2331–2386.
66 L. N. Munuhe, E. S. Madivoli, D. M. Nzilu, P. N. Lemeitaron and P. K. Kimani, *J. Chem.*, 2025, **2025**, 4477822.
67 Z. Abdullah and S. Ahmed, *Environ. Sci.: Water Res. Technol.*, 2025, **11**, 1428–1445.
68 M. M. Ghangrekar and P. Chatterjee, *Carbon Nanotubes for Clean Water*, ed. R. Das, Springer International Publishing, Cham, 2018, pp. 11–26, DOI: 10.1007/978-3-319-95603-9_2.
69 S. S. Ray, R. Gusain and N. Kumar, *Carbon Nanomaterial-Based Adsorbents for Water Purification: Fundamentals and Applications*, Elsevier, 2020.
70 H. Ali, E. Khan and I. Ilahi, *J. Chem.*, 2019, **2019**, 6730305.
71 L. Järup, *Br. Med. Bull.*, 2003, **68**, 167–182.
72 M. Patel, R. Kumar, K. Kishor, T. Mlsna, C. U. Pittman Jr and D. Mohan, *Chem. Rev.*, 2019, **119**, 3510–3673.
73 Q. Qing Li, A. Loganath, Y. Seng Chong, J. Tan and J. Philip Obbard, *J. Toxicol. Environ. Health, Part A*, 2006, **69**, 1987–2005.
74 S. Rojas and P. Horcajada, *Chem. Rev.*, 2020, **120**, 8378–8415.
75 V. K. Parida, N. Singh, M. Priyadarshini, P. Kumari, D. Datta and A. Tambi, *J. Ind. Eng. Chem.*, 2025, **150**, 247–264.
76 J. Lin, W. Ye, M. Xie, D. H. Seo, J. Luo, Y. Wan and B. Van der Bruggen, *Nat. Rev. Earth Environ.*, 2023, **4**, 785–803.
77 J. O. Osuoha, B. O. Anyanwu and C. Ejileugha, *J. Hazard. Mater. Adv.*, 2023, **9**, 100206.
78 M. Farhan Hanafi and N. Sapawe, *Mater. Today: Proc.*, 2020, **31**, A141–A150.
79 W. Zhou, M. Li and V. Achal, *Emerging Contam.*, 2025, **11**, 100410.
80 P. Durgadevi, K. Girigoswami, K. Harini, A. Thirumalai, V. Kiran and A. Girigoswami, *Toxicol. Environ. Health Sci.*, 2025, **17**, 23–49.
81 Y. Feng, Z. Li and W. Li, *Nat. Prod. Commun.*, 2025, **20**, 1934578X241311451.
82 X. Zhou, X. Zhou, C. Wang and H. Zhou, *Chemosphere*, 2023, **313**, 137489.
83 A. Mangotra and S. K. Singh, *J. Biotechnol.*, 2024, **382**, 51–69.
84 A. Efstratiou, J. E. Ongerth and P. Karanis, *Water Res.*, 2017, **114**, 14–22.
85 N. M. Ali, M. K. Khan, B. Mazhar and M. Mustafa, *Discover Water*, 2025, **5**, 19.
86 A. Igwaran, A. J. Kayode, K. M. Moloantoa, Z. P. Khetsha and J. O. Unuofin, *Water, Air, Soil Pollut.*, 2024, **235**, 71.
87 A. M. Thawabteh, H. A. Naseef, D. Karaman, S. A. Bufo, L. Scrano and R. Karaman, *Toxins*, 2023, **15**, 582.
88 N. J. Ashbolt, *Curr. Environ. Health Rep.*, 2015, **2**, 95–106.
89 M. Kumar, S. Sridharan, A. D. Sawarkar, A. Shakeel, P. Anerao, G. Mannina, P. Sharma and A. Pandey, *Sci. Total Environ.*, 2023, **859**, 160031.
90 H. J. Tyc, K. Kłodnicka, B. Teresińska, R. Karpiński, J. Flieger and J. Baj, *Int. J. Mol. Sci.*, 2025, **26**, 6156.
91 Z. S. Thin, R. A. Raja Ali and L. T. Gew, *Toxicol. Environ. Health Sci.*, 2025, DOI: 10.1007/s13530-025-00269-5.
92 J. O. Tijani, O. O. Fatoba, O. O. Babajide and L. F. Petrik, *Environ. Chem. Lett.*, 2016, **14**, 27–49.
93 N. P. Ivleva, *Chem. Rev.*, 2021, **121**, 11886–11936.
94 L. Wang, H. Wang, C. Tizaoui, Y. Yang, J. Ali and W. Zhang, *Sens. Diagn.*, 2023, **2**, 46–77.
95 T. Matos, M. S. Martins, R. Henriques and L. M. Goncalves, *J. Water Process Eng.*, 2024, **64**, 105624.
96 P. Gernez, V. Lafon, A. Lerouxel, C. Curti, B. Lubac, S. Cerisier and L. Barillé, *Remote Sens.*, 2015, **7**, 9507–9528.
97 R. E. A. Mohammad, S. Veerasingam, G. Suresh, S. Rajendran, K. K. Sadasivuni, S. Ghani and F. Al-Khayat, *Chem. Eng. J. Adv.*, 2025, **23**, 100802.
98 G. S. Bilotta and R. E. Brazier, *Water Res.*, 2008, **42**, 2849–2861.
99 S. S. Kaushal, P. M. Groffman, G. E. Likens, K. T. Belt, W. P. Stack, V. R. Kelly, L. E. Band and G. T. Fisher, *Proc. Natl. Acad. Sci. U. S. A.*, 2005, **102**, 13517–13520.
100 V. K. Gupta, P. J. M. Carrott, M. M. L. Ribeiro Carrott and Suhas, *Crit. Rev. Environ. Sci. Technol.*, 2009, **39**, 783–842.
101 Y.-F. Zhou and R. J. Haynes, *Crit. Rev. Environ. Sci. Technol.*, 2010, **40**, 909–977.
102 T. R. Sahoo and B. Prelot, *Nanomaterials for the Detection and Removal of Wastewater Pollutants*, ed. B. Bonelli, F. S. Freyria, I. Rossetti and R. Sethi, Elsevier, 2020, pp. 161–222, DOI: 10.1016/B978-0-12-818489-9.00007-4.
103 A. Srivastava, P. K. Meena, P. M. Patane, D. Meena, S. Shelare and C. S. Wagle, *Biofuels*, 2025, 1–16, DOI: 10.1080/17597269.2025.2517454.
104 M. Ahmaruzzaman, *Adv. Colloid Interface Sci.*, 2011, **166**, 36–59.
105 G. Crini, *Prog. Polym. Sci.*, 2005, **30**, 38–70.
106 R. Chakraborty, A. Asthana, A. K. Singh, B. Jain and A. B. H. Susan, *Int. J. Environ. Anal. Chem.*, 2022, **102**, 342–379.
107 K. M. AlAqad, M. M. Abdelnaby, A. Tanimu, I. Abdulazeez and A. M. Elsharif, *Environ. Pollut. Manage.*, 2025, **2**, 1–13.
108 M. M. Nasr, P. Rezvani, H. Rashedi, F. Yazdian, M. Pourmadadi, A. Rahdar, S. Fathi-karkan and S. Pandey, *Cellulose*, 2025, **32**, 6363–6397.
109 M. Hussain, A. Riaz, H. Zeb, A. Ali, R. Mujahid, F. Ahmad and M. S. Zafar, *J. Water Process Eng.*, 2025, **71**, 107333.
110 G. George, A. M. Ealias and M. P. Saravanakumar, *Environ. Sci. Pollut. Res.*, 2024, **31**, 12748–12779.
111 A. Mary Ealias, G. Meda and K. Tanzil, *Rev. Environ. Contam. Toxicol.*, 2024, **262**, 16.
112 H. Kolya and C.-W. Kang, *Discover Water*, 2025, **5**, 28.
113 P. Mehta, D. K. Chelike and R. K. Rathore, *ChemistrySelect*, 2024, **9**, e202400959.
114 C. Chen, L. Shen, B. Wang, X. Lu, S. Raza, J. Xu, B. Li, H. Lin and B. Chen, *Chem. Soc. Rev.*, 2025, **54**, 2208–2245.
115 I. Ali, *Sep. Purif. Rev.*, 2010, **39**, 95–171.
116 H. Han, M. K. Rafiq, T. Zhou, R. Xu, O. Mašek and X. Li, *J. Hazard. Mater.*, 2019, **369**, 780–796.
117 T. Luukkonen and J. Teeriniemi, *iScience*, 2025, **28**, 112993.
118 Y. Qi, S. Zhao, Y. Shen, X. Jiang, H. Lv, C. Han, W. Liu and Q. Zhao, *Catalysts*, 2024, **14**, 575.
119 G. Crini, *Bioresour. Technol.*, 2006, **97**, 1061–1085.

120 W. S. Chai, J. Y. Cheun, P. S. Kumar, M. Mubashir, Z. Majeed, F. Banat, S.-H. Ho and P. L. Show, *J. Cleaner Prod.*, 2021, **296**, 126589.
121 S. Chowdhury and R. Balasubramanian, *Adv. Colloid Interface Sci.*, 2014, **204**, 35–56.
122 S. Bhattacharyya, R. Raju, U. Roy and P. Kumar, *Prog. Eng. Sci.*, 2025, **2**, 100107.
123 A. Alam, A. Hassan and N. Das, *Prog. Mater. Sci.*, 2026, **155**, 101528.
124 M. Gomez-Suarez, Y. Chen and J. Zhang, *Polym. Chem.*, 2023, **14**, 4000–4032.
125 Z. Xia, Y. Zhao and S. B. Darling, *Adv. Mater. Interfaces*, 2021, **8**, 2001507.
126 M. He, S. Shi, Z. Liu, Y. Wu and L. Wang, *Chem. Commun.*, 2025, **61**, 5072–5083.
127 L. Huang, R. Liu, J. Yang, Q. Shuai, B. Yuliarto, Y. V. Kaneti and Y. Yamauchi, *Chem. Eng. J.*, 2021, **408**, 127991.
128 S. Yu, H. Pang, S. Huang, H. Tang, S. Wang, M. Qiu, Z. Chen, H. Yang, G. Song, D. Fu, B. Hu and X. Wang, *Sci. Total Environ.*, 2021, **800**, 149662.
129 B. Samiey, C.-H. Cheng and J. Wu, *Materials*, 2014, **7**, 673–726.
130 Z.-y. Han, L.-j. Huang, H.-j. Qu, Y.-x. Wang, Z.-j. Zhang, Q.-l. Rong, Z.-q. Sang, Y. Wang, M. J. Kipper and J.-g. Tang, *J. Mater. Sci.*, 2021, **56**, 9545–9574.
131 B. Qiu, Q. Shao, J. Shi, C. Yang and H. Chu, *Sep. Purif. Technol.*, 2022, **300**, 121925.
132 G. P. Udayakumar, S. Muthusamy, B. Selvaganesh, N. Sivarajasekar, K. Rambabu, S. Sivamani, N. Sivakumar, J. P. Maran and A. Hosseini-Bandegharaei, *Biotechnol. Adv.*, 2021, **52**, 107815.
133 A. Das, T. Ringu, S. Ghosh and N. Pramanik, *Polym. Bull.*, 2023, **80**, 7247–7312.
134 T. Russo, P. Fucile, R. Giacometti and F. Sannino, *Processes*, 2021, **9**, 719.
135 E. Khademian, E. Salehi, H. Sanaeepur, F. Galiano and A. Figoli, *Sci. Total Environ.*, 2020, **738**, 139829.
136 L. Fu, J. Li, G. Wang, Y. Luan and W. Dai, *Ecotoxicol. Environ. Saf.*, 2021, **217**, 112207.
137 T. M. Gür, *Prog. Energy Combust. Sci.*, 2022, **89**, 100965.
138 A. Dąbrowski, *Adv. Colloid Interface Sci.*, 2001, **93**, 135–224.
139 R. I. Yousef, B. El-Eswed and A. a. H. Al-Muhtaseb, *Chem. Eng. J.*, 2011, **171**, 1143–1149.
140 A. Gupta, V. Sharma, K. Sharma, V. Kumar, S. Choudhary, P. Mankotia, B. Kumar, H. Mishra, A. Moulick and A. Ekielski, *Materials*, 2021, **14**, 4702.
141 A. Gupta, V. Sharma, K. Sharma, V. Kumar, S. Choudhary, P. Mankotia, B. Kumar, H. Mishra, A. Moulick, A. Ekielski and P. K. Mishra, *Materials*, 2021, **14**, 4702.
142 T. Alsawy, E. Rashad, M. El-Qelish and R. H. Mohammed, *npj Clean Water*, 2022, **5**, 29.
143 G. Z. Kyzas, E. A. Deliyanni, K. A. Matis, N. K. Lazaridis, D. N. Bikiaris and A. C. Mitropoulos, *Compos. Interfaces*, 2018, **25**, 415–454.
144 G. L. Dotto and G. McKay, *J. Environ. Chem. Eng.*, 2020, **8**, 103988.
145 M. E. González-López, C. M. Laureano-Anzaldo, A. A. Pérez-Fonseca, M. Arellano and J. R. Robledo-Ortíz, *Sep. Purif. Rev.*, 2022, **51**, 358–372.
146 A. Sherikar, S. More, M. U. M. Siddique, Y. O. Agarwal, A. Ansari, V. R. Askari, R. R. Zairov, T. M. Aminabhavi, M. S. Hasnain, B. B. Panda and A. K. Nayak, *Natural Biopolymers for Drug Delivery*, ed. A. K. Nayak, M. S. Hasnain and T. M. Aminabhavi, Woodhead Publishing, 2025, pp. 1–28, DOI: **10.1016/B978-0-323-95367-2.00025-9**.
147 Y. Sun, Y. Bai, W. Yang, K. Bu, S. K. Tanveer and J. Hai, *Front. Chem.*, 2022, **10**, 2022.
148 P. R. Yaashikaa, P. Senthil Kumar and S. Karishma, *Environ. Res.*, 2022, **212**, 113114.
149 P. Kanmani, J. Aravind, M. Kamaraj, P. Sureshbabu and S. Karthikeyan, *Bioresour. Technol.*, 2017, **242**, 295–303.
150 E. Sohouli, N. Irannejad, A. Ziarati, H. Ehrlich, M. Rahimi-Nasrabadi, F. Ahmadi and R. Luque, *Environ. Chem. Lett.*, 2022, **20**, 3789–3809.
151 S. Jagota, S. S. Pandey, M. Hakkarainen, P. Chandra, M. Yadav, S. G. Warkar and A. Sand, *ChemistrySelect*, 2025, **10**, e02854.
152 L. V. Lawrence and D. Vishnu, *J. Environ. Manage.*, 2025, **388**, 126012.
153 T. Biswal, *Advances in Nanomaterials for Detection, Control, and Removal of Environmental Pollutants*, ed. A. K. Singh, A. K. Singh and M. A. B. H. Susan, Springer Nature Switzerland, Cham, 2025, pp. 65–85, DOI: **10.1007/978-3-031-87409-3_3**.
154 K. Z. Elwakeel, A. M. Elgarahy, Z. A. Khan, M. S. Almughamisi and A. S. Al-Bogami, *Mater. Adv.*, 2020, **1**, 1546–1574.
155 S. Lal and S. Bhatnagar, *Curr. Mater. Sci.*, 2025, **18**, 149–167.
156 J. Odoom, O. T. Iorhemen and J. Li, *Energy Ecol. Environ.*, 2025, **10**, 15–44.
157 X. Xiong, J. Liu, T. Xiao, K. Lin, Y. Huang, P. Deng, H. Hu and J. Wang, *Biochar*, 2025, **7**, 41.
158 A. M. Shabbirahmed, A. Jacob, P. Dey, P. Somu and D. Haldar, *Discover Appl. Sci.*, 2025, **7**, 771.
159 G. R. Mavlankar, M. N. Bhatu, P. P. Baikar and S. P. Patil, *ChemistrySelect*, 2024, **9**, e202402065.
160 M. Jonoobi, R. Oladi, Y. Davoudpour, K. Oksman, A. Dufresne, Y. Hamzeh and R. Davoodi, *Cellulose*, 2015, **22**, 935–969.
161 Suhas, V. K. Gupta, P. J. M. Carrott, R. Singh, M. Chaudhary and S. Kushwaha, *Bioresour. Technol.*, 2016, **216**, 1066–1076.
162 A. Darmenbayeva, R. Rajasekharan, B. Massalimova, N. Bektenov, R. Taubayeva, K. Bazarbaeva, M. Kurmanaliev, Z. Mukazhanova, A. Nurlybayeva, K. Bulekbayeva, A. Kabylbekova and A. Ungarbayeva, *Molecules*, 2024, **29**, 5969.
163 Y. Zhou, M. Zhang, X. Hu, X. Wang, J. Niu and T. Ma, *J. Chem. Eng. Data*, 2013, **58**, 413–421.
164 C. Wang and S. Okubayashi, *Carbohydr. Polym.*, 2019, **225**, 115248.
165 S. Bo, W. Ren, C. Lei, Y. Xie, Y. Cai, S. Wang, J. Gao, Q. Ni and J. Yao, *J. Solid State Chem.*, 2018, **262**, 135–141.

166 J. Wang, L. Dai, J. Cheng, L.-H. Deng and J. He, *Desalin. Water Treat.*, 2016, **57**, 5821–5827.
167 Z. Karim, M. Hakalahti, T. Tammelin and A. P. Mathew, *RSC Adv.*, 2017, **7**, 5232–5241.
168 T. Hu, Q. Liu, Q. Liu, Y. Wu, C. Qiao and J. Yao, *Carbohydr. Polym.*, 2019, **209**, 291–298.
169 T. Shahnaz, V. Sharma, S. Subbiah and S. Narayanasamy, *J. Water Process Eng.*, 2020, **36**, 101283.
170 A. S. Wittmar, D. Baumert and M. Ulbricht, *Macromol. Mater. Eng.*, 2021, **306**, 2000778.
171 X. Luo, J. Zeng, S. Liu and L. Zhang, *Bioresour. Technol.*, 2015, **194**, 403–406.
172 A. Alipour, S. Zarinabadi, A. Azimi and M. Mirzaei, *Int. J. Biol. Macromol.*, 2020, **151**, 124–135.
173 J. Lu, R.-N. Jin, C. Liu, Y.-F. Wang and X.-K. Ouyang, *Int. J. Biol. Macromol.*, 2016, **93**, 547–556.
174 Z. Tan, B. Yang, W. Liu, D. Yang, X. Qiu and D. Zheng, *Carbohydr. Polym.*, 2025, **348**, 122890.
175 F. Olivito, V. Algieri, A. Jiritano, M. A. Tallarida, A. Tursi, P. Costanzo, L. Maiuolo and A. De Nino, *RSC Adv.*, 2021, **11**, 34309–34318.
176 Y. Wang, H. Wang, H. Peng, Z. Wang, J. Wu and Z. Liu, *Fibers Polym.*, 2018, **19**, 340–349.
177 S. Gopi, A. Pius, R. Kargl, K. S. Kleinschek and S. Thomas, *Polym. Bull.*, 2019, **76**, 1557–1571.
178 L. d. Kunz Lazzari, D. Perondi, A. J. Zattera and R. M. Campomanes Santana, *Langmuir*, 2021, **37**, 3180–3188.
179 S. Bo, W. Ren, C. Lei, Y. Xie, Y. Cai, S. Wang, J. Gao, Q. Ni and J. Yao, *J. Solid State Chem.*, 2018, **262**, 135–141.
180 A. S. M. Wittmar, D. Baumert and M. Ulbricht, *Macromol. Mater. Eng.*, 2021, **306**, 2000778.
181 H. Y. Zhu, Y. Q. Fu, R. Jiang, J. H. Jiang, L. Xiao, G. M. Zeng, S. L. Zhao and Y. Wang, *Chem. Eng. J.*, 2011, **173**, 494–502.
182 X. Luo, X. Lei, N. Cai, X. Xie, Y. Xue and F. Yu, *ACS Sustain. Chem. Eng.*, 2016, **4**, 3960–3969.
183 X. Sun, L. Yang, Q. Li, J. Zhao, X. Li, X. Wang and H. Liu, *Chem. Eng. J.*, 2014, **241**, 175–183.
184 X. Yu, D. Kang, Y. Hu, S. Tong, M. Ge, C. Cao and W. Song, *RSC Adv.*, 2014, **4**, 31362–31369.
185 Y. Wang, H. Wang, H. Peng, Z. Wang, J. Wu and Z. Liu, *Fibers Polym.*, 2018, **19**, 340–349.
186 S. Gopi, A. Pius, R. Kargl, K. S. Kleinschek and S. Thomas, *Polym. Bull.*, 2019, **76**, 1557–1571.
187 D.-M. Guo, Q.-D. An, Z.-Y. Xiao, S.-R. Zhai and D.-J. Yang, *Carbohydr. Polym.*, 2018, **202**, 306–314.
188 M. E. A. Ali, *Arabian J. Chem.*, 2018, **11**, 1107–1116.
189 X. Chen, W. Zhang, X. Luo, F. Zhao, Y. Li, R. Li and Z. Li, *Chemosphere*, 2017, **185**, 991–1000.
190 F. Marrakchi, W. Khanday, M. Asif and B. Hameed, *Int. J. Biol. Macromol.*, 2016, **93**, 1231–1239.
191 S. Chatterjee, T. Chatterjee and S. H. Woo, *Chem. Eng. J.*, 2011, **166**, 168–175.
192 Y. Li, H. Gao, C. Wang, X. Zhang and H. Zhou, *Int. J. Biol. Macromol.*, 2018, **117**, 30–41.
193 A. Rajeswari, A. Amalraj and A. Pius, *J. Water Process Eng.*, 2016, **9**, 123–134.
194 M. Rajeswari, R. Seenivasagan, P. Prabhakaran, S. Rajakumar and P. M. Ayyasamy, *J. Water Process Eng.*, 2016, **13**, 189–195.
195 X. Yang, Y. Li, H. Gao, C. Wang, X. Zhang and H. Zhou, *Int. J. Biol. Macromol.*, 2018, **117**, 30–41.
196 J. H. Chen, H. Lin, Z. H. Luo, Y. S. He and G. P. Li, *Desalination*, 2011, **277**, 265–273.
197 Y.-Y. Wang, W.-B. Yao, Q.-W. Wang, Z.-H. Yang, L.-F. Liang and L.-Y. Chai, *Trans. Nonferrous Met. Soc. China*, 2016, **26**, 2230–2237.
198 Y. Yan, Q. An, Z. Xiao, W. Zheng and S. Zhai, *Chem. Eng. J.*, 2017, **313**, 475–486.
199 Y. Wang, Y. Feng, X.-F. Zhang, X. Zhang, J. Jiang and J. Yao, *J. Colloid Interface Sci.*, 2018, **514**, 190–198.
200 Z.-J. Shao, X.-L. Huang, F. Yang, W.-F. Zhao, X.-Z. Zhou and C.-S. Zhao, *Carbohydr. Polym.*, 2018, **187**, 85–93.
201 Y. Feng, H. Wang, J. Xu, X. Du, X. Cheng, Z. Du and H. Wang, *J. Hazard. Mater.*, 2021, **416**, 125777.
202 M. Nasrollahzadeh, M. Sajjadi, S. Iravani and R. S. Varma, *Carbohydr. Polym.*, 2021, **251**, 116986.
203 M. Gholinejad, F. Saadati, S. Shaybanizadeh and B. Pullithadathil, *RSC Adv.*, 2016, **6**, 4983–4991.
204 L. Guo, G. Li, J. Liu, Y. Meng and Y. Tang, *Carbohydr. Polym.*, 2013, **93**, 374–379.
205 P. N. Singh, D. Tiwary and I. Sinha, *J. Environ. Chem. Eng.*, 2014, **2**, 2252–2258.
206 I. Ihsanullah, M. Bilal and A. Jamal, *Chem. Rec.*, 2022, **22**, e202100312.
207 A. Pourjavadi, A. Abedin-Moghanaki and A. Tavakoli, *RSC Adv.*, 2016, **6**, 38042–38051.
208 H. Hosseinzadeh and S. Ramin, *Int. J. Biol. Macromol.*, 2018, **106**, 101–115.
209 J. Guo, J. Wang, G. Zheng and X. Jiang, *Environ. Sci. Pollut. Res.*, 2019, **26**, 24395–24406.
210 M. Dai, Y. Liu, B. Ju and Y. Tian, *Bioresour. Technol.*, 2019, **294**, 122192.
211 F. Haq, H. Yu, Y. Wang, L. Wang, M. Haroon, A. Khan, S. Mehmood and T. Lin, *J. Mol. Struct.*, 2020, **1207**, 127752.
212 F. Hayeeye, Q. J. Yu, M. Sattar, W. Chinpa and O. Sirichote, *Adsorpt. Sci. Technol.*, 2018, **36**, 355–371.
213 X. Wang, K. Huang, Y. Chen, J. Liu, S. Chen, J. Cao, S. Mei, Y. Zhou and T. Jing, *J. Hazard. Mater.*, 2018, **350**, 46–54.
214 J. Meng, X. Lin, H. Li, Y. Zhang, J. Zhou, Y. Chen, R. Shang and X. Luo, *RSC Adv.*, 2019, **9**, 8091–8103.
215 P. Herman, I. Fábián and J. Kalmár, *ACS Appl. Nano Mater.*, 2020, **3**, 195–206.
216 A. Dolgormaa, C.-j. Lv, Y. Li, J. Yang, J.-x. Yang, P. Chen, H.-p. Wang and J. Huang, *Molecules*, 2018, **23**, 2982.
217 K. Kaur and R. Jindal, *Carbohydr. Polym.*, 2019, **207**, 398–410.
218 B. Che, H. Li, D. Zhou, Y. Zhang, Z. Zeng, C. Zhao, C. He, E. Liu and X. Lu, *Composites, Part B*, 2019, **165**, 671–678.
219 S. Saber-Samandari, S. Saber-Samandari, H. Joneidi-Yekta and M. Mohseni, *Chem. Eng. J.*, 2017, **308**, 1133–1144.
220 A. A. Haroun, H. M. Mashaly and N. H. El-Sayed, *Clean Technol. Environ.*, 2013, **15**, 367–374.

221 M. Sabzi, N. Shafagh and M. Mohammadi, *J. Appl. Polym. Sci.*, 2019, **136**, 48266.
222 J. Jiang, Q. Zhang, X. Zhan and F. Chen, *Chem. Eng. J.*, 2019, **358**, 1539–1551.
223 M. Nagpal and R. Kakkar, *Res. Chem. Intermed.*, 2020, **46**, 2497–2521.
224 M. Nagpal and R. Kakkar, *ChemistrySelect*, 2020, **5**, 1235–1246.
225 B. Li, F. Zhou, K. Huang, Y. Wang, S. Mei, Y. Zhou and T. Jing, *Sci. Rep.*, 2016, **6**, 33573.
226 S. Lapwanit, T. Sooksimuang and T. Trakulsujaritchok, *J. Environ. Chem. Eng.*, 2018, **6**, 6221–6230.
227 S. Jo, Y. Oh, S. Park, E. Kan and S. H. Lee, *Biotechnol. Bioprocess Eng.*, 2017, **22**, 734–738.
228 M. Dargahi, H. Ghasemzadeh and A. Torkaman, *Polym. Bull.*, 2019, **76**, 5039–5058.
229 K. R. Singh and K. M. Poluri, *Environ. Res.*, 2023, **231**, 116145.
230 M. Yang, X. Liu, Y. Qi, W. Sun and Y. Men, *J. Colloid Interface Sci.*, 2017, **506**, 669–677.
231 Y. Zheng, J. Yang, R. Yang, A. Wang, B. Deng, F. Peng, Y. Peng, L. He and L. Fu, *Dig. J. Nanomater. Biostruct.*, 2015, **10**, 349–357.
232 H. Agougui, M. Jabli and H. Majdoub, *J. Appl. Polym. Sci.*, 2017, **134**, 45385.
233 M. H. Karimi, G. R. Mahdavinia, B. Massoumi, A. Baghban and M. Saraei, *Int. J. Biol. Macromol.*, 2018, **113**, 361–375.
234 S. F. Soares, T. R. Simoes, T. Trindade and A. L. Daniel-da-Silva, *Water, Air, Soil Pollut.*, 2017, **228**, 1–11.
235 G. R. Mahdavinia and A. Mosallanezhad, *J. Water Process Eng.*, 2016, **10**, 143–155.
236 H. Hosseinzadeh, *Pol. J. Chem. Technol.*, 2015, **17**, 70–76.
237 G. R. Mahdavinia and A. Asgari, *Polym. Bull.*, 2013, **70**, 2451–2470.
238 A. Pourjavadi, M. Doulabi and M. Doroudian, *J. Iran. Chem. Soc.*, 2014, **11**, 1057–1065.
239 X. Liang, J. Duan, Q. Xu, X. Wei, A. Lu and L. Zhang, *Chem. Eng. J.*, 2017, **317**, 766–776.
240 S. Choudhury and S. K. Ray, *Carbohydr. Polym.*, 2018, **200**, 305–320.
241 F. H. H. Abdellatif and M. M. Abdellatif, *Cellulose*, 2020, **27**, 441–453.
242 O. Duman, T. G. Polat, C. Ö. Diker and S. Tunç, *Int. J. Biol. Macromol.*, 2020, **160**, 823–835.
243 T. Qiang, Q. Bu, L. Ren and X. Wang, *J. Appl. Polym. Sci.*, 2014, **131**, 40285.
244 T. Qiang, M. Luo, Q. Bu and X. Wang, *Chem. Eng. J.*, 2012, **197**, 343–349.
245 P. Thanikaivelan, N. T. Narayanan, B. K. Pradhan and P. M. Ajayan, *Sci. Rep.*, 2012, **2**, 230.
246 J. Li, Z. Guo, S. Zhang and X. Wang, *Chem. Eng. J.*, 2011, **172**, 892–897.
247 Y. Zhang, S. Ni, X. Wang, W. Zhang, L. Lagerquist, M. Qin, S. Willför, C. Xu and P. Fatehi, *Chem. Eng. J.*, 2019, **372**, 82–91.
248 B. Xie, Y. Hou and Y. Li, *BioResources*, 2021, **16**, 249.
249 T. Das, A. Kumar, J. Saji, A. Pandey and D. K. Patel, *ACS Sustainable Resour. Manage.*, 2024, **1**, 141–153.
250 S. Patra, E. Roy, R. Madhuri and P. K. Sharma, *J. Ind. Eng. Chem.*, 2016, **33**, 226–238.
251 C. Cheng, Y. Cai, G. Guan, L. Yeo and D. Wang, *Angew. Chem., Int. Ed.*, 2018, **57**, 11177–11181.
252 L. Chen, Y. Li, Q. Du, Z. Wang, Y. Xia, E. Yedinak, J. Lou and L. Ci, *Carbohydr. Polym.*, 2017, **155**, 345–353.